

# Identifying Latent Stochastic Differential Equations with Variational Auto-Encoders

Ali Hasan,<sup>1\*</sup> João M. Pereira,<sup>2\*</sup> Sina Farsiu,<sup>1,2</sup> Vahid Tarokh<sup>2</sup>

<sup>1</sup>Department of Biomedical Engineering, Duke University

<sup>2</sup>Department of Electrical and Computer Engineering, Duke University  
 {ali.hasan, joao.pereira, sina.farsiu, vahid.tarokh}@duke.edu

## Abstract

We present a method for learning latent stochastic differential equations (SDEs) from high dimensional time series data. Given a time series generated from a lower dimensional Itô process, the proposed method uncovers the relevant coefficients of the SDE through a self-supervised learning approach. Using the framework of variational autoencoders (VAEs), we consider a conditional generative model for the data based on the Euler-Maruyama approximation of SDE solutions. Furthermore, we use recent results on identifiability of semi-supervised learning to show that the proposed model can recover not only the underlying SDE coefficients, but also the original latent space, up to an isometry, in the limit of infinite data. We validate the model through a series of different simulated video processing tasks where the underlying SDE is known. Our results suggest that the proposed method effectively learns the underlying SDE, as predicted by the theory.

## 1 Introduction

Variational auto-encoders (VAEs) are a widely used tool to learn lower-dimensional latent representations of high-dimensional data. However, the learned latent representations often lack interpretability, and it is challenging to extract relevant information from the representation of the dataset in the latent space. In particular, when the high-dimensional data is governed by unknown and lower-dimensional dynamics, arising, for instance, from unknown physical or biological interactions, the latent space representation often fails to bring insight on these dynamics.

We propose a VAE-based framework for recovering latent dynamics governed by stochastic differential equations (SDEs). Our motivation for using SDEs is that they are already often used to model physical and biological phenomena, to study financial markets, and their properties have been extensively studied in the fields of probability and statistics. We believe this method can be useful in describing trajectories of high dimensional data with underlying physical or biological dynamics, with applications such as video data, longitudinal medical data or gene regulatory dynamics.

Suppose we observe a high-dimensional time-series  $\{X_t\}_{t \in \mathcal{T}}$ , for which there exists a (typically lower dimensional) latent representation  $\{Z_t\}_{t \in \mathcal{T}}$ . Specifically, there exists a decoder  $f$  and an encoder  $\psi$  such that

$$X_t = f(Z_t) \quad \text{and} \quad Z_t = \psi(X_t), \quad t \in \mathcal{T} \quad (1)$$

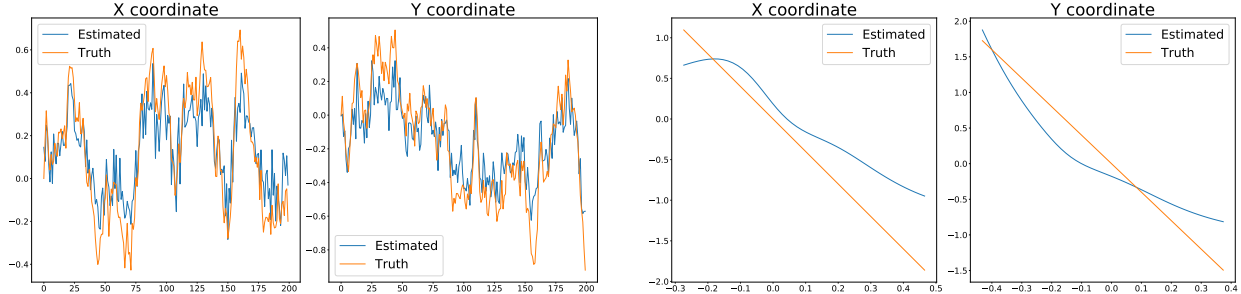
where  $f$ ,  $\psi$  and  $Z_t$  are unknown. Moreover,  $Z_t$  is assumed to be governed by an SDE, with coefficients that are also unknown. In this paper we propose a VAE-based model for recovering both the latent representation ( $f$  and  $\psi$ ) and the coefficients of the SDE that governs  $Z_t$ .

We are also concerned with identifiability. In this regard, we propose the following twofold approach.

- (i) Under some conditions over the diffusion coefficient of  $Z_t$ , we show there exists  $\tilde{f}$ ,  $\tilde{\psi}$  and  $\tilde{Z}_t$  which are also a solution of (1), and  $\tilde{Z}_t$  is governed by an SDE with an isotropic diffusion coefficient (Theorem 2).



(a) Yellow ball moving according to a 2D Ornstein-Uhlenbeck process;



(b) Comparison between the true centers of the ball and the latent representation learned by the VAE at different frames of the video;

(c) Comparison between the true drift coefficient and the drift coefficient estimated by the VAE;

Figure 1: From a video of a yellow ball moving in the plane, according to a 2D Ornstein-Uhlenbeck process (Figure 1(a)), the proposed model learns that the relevant latent representation of each frame are the  $x$  and  $y$  coordinates of the ball (Figure 1(b)), and learns the drift coefficient of the SDE (Figure 1(c)).

- (ii) We prove that the method proposed in this paper, in the limit of infinite data, is able to recover, up to an isometry,  $\tilde{f}$ ,  $\tilde{\psi}$  and the drift coefficient of the  $\tilde{Z}_t$  (Theorems 3 and 4).

In other words, (i) implies that, from all possible triplets  $(\tilde{f}, \tilde{\psi}, \tilde{Z}_t)$  that fit the data, there is one for which  $\tilde{Z}_t$  is governed by an SDE with an isotropic diffusion coefficient, and (ii) guarantees we find this triplet in the limit of infinite data. This makes it simpler to learn the latent dynamics, since the diffusion coefficient does not need to be estimated. An example of the proposed method is presented in Figure 1.

Our paper is organized as follows. First, we present an overview of previous work. Then we formalize the notion of SDEs, develop a generative model to study latent SDEs and present the VAE framework that enables learning of the proposed model. Followingly, we show that the VAE proposed recovers the true model parameters up to an isometry and give some practical considerations on the method presented. Finally, we test the proposed method in several datasets and present a brief discussion on the results.

## 2 Related Work

Previous work in learning SDEs has been mostly focused on lower-dimensional data. Classical approaches assume fixed drift and diffusion coefficients with parameters that need to be estimated [1].

In [2], a method is proposed where the terms of the Fokker-Planck equation are estimated using sparse regression with a predefined dictionary of functions, and in [3] a similar idea is applied to the Kramers-Moyal expansion of the SDE.

More recently, in [4], the adjoint sensitivity method is used for recovering latent SDE, and although the datasets analyzed have higher dimensions than previous approaches, they cannot still be considered high-dimensional. In [5], a method is presented for uncovering the latent SDE for high-dimensional data, however the map from the data to the latent space is assumed to be linear. In [6], a method using variational auto-encoders is presented to recover latent second-order ordinary differential equations from data, and it can also be used to recover data with stochastic latent dynamics, such as SDEs.

Finally, in the case of image/video data, recent works in stochastic video prediction [7,8] describe methods for stochastic predictions of video. While these are favorable on reproducing the dynamics of the observed data, the latent variables lack interpretability. In [9], a method based on recurrent neural networks is presented that decomposes the latent space and promotes disentanglement, in an effort to provide more meaningful features in the latent space.

### 3 Stochastic Differential Equations

Here we formalize the notion of SDE. For a time interval  $\mathbb{T} = [0, T]$ , let  $\{W_t\}_{t \in \mathbb{T}}$  be a  $d$ -dimensional Wiener process. We say the stochastic process  $\{Z_t\}_{t \in \mathbb{T}} \in \mathbb{R}^d$  is a solution to the Itô SDE

$$dZ_t = \mu(Z_t, t) dt + \sigma(Z_t, t) dW_t, \quad (2)$$

if  $Z_0$  is independent of the  $\sigma$ -algebra generated by  $W_t$ , and

$$Z_T = Z_0 + \int_0^T \mu(Z_t, t) dt + \int_0^T \sigma(Z_t, t) dW_t. \quad (3)$$

Here we denote the *drift coefficient* by  $\mu : \mathbb{R}^d \times \mathbb{T} \rightarrow \mathbb{R}^d$ , the *diffusion coefficient* by  $\sigma : \mathbb{R}^d \times \mathbb{T} \rightarrow \mathbb{R}^{d \times d}$  and the second integral in (3) is the Itô stochastic integral [10]. When the coefficients are globally Lipschitz, that is,

$$\begin{aligned} \|\mu(x, t) - \mu(y, t)\| + \|\sigma(x, t) - \sigma(y, t)\| &\leq D\|x - y\| \\ \forall x, y \in \mathbb{R}^d, t \in \mathbb{T}, \end{aligned} \quad (4)$$

for some constant  $D > 0$ , there exists a unique  $t$ -continuous strong solution to (2) [10, Theorem 5.2.1]. Finally, throughout the paper we can assume  $\sigma(z, t)$  is a symmetric positive semi-definite matrix for all  $z \in \mathbb{R}^d$  and  $t \in \mathbb{T}$ , this follows from [10, Theorem 7.3.3].

### 4 Problem Definition

In this paper, we consider a high-dimensional stochastic process  $\{X_t\}_{t \in \mathbb{T}} \in \mathbb{R}^n$ , which has a latent representation  $\{Z_t\}_{t \in \mathbb{T}} \in \mathbb{R}^d$ , with  $n \geq d$ , that is, there exists a decoder  $f : \mathbb{R}^d \rightarrow \mathbb{R}^n$  and an encoder  $\psi : \mathbb{R}^n \rightarrow \mathbb{R}^d$  such that (1) holds. In particular, this implies  $f$  is injective and  $\psi \equiv f^{-1}$ . Moreover,  $Z_t$  is governed by an SDE, with drift coefficient  $\mu : \mathbb{R}^d \rightarrow \mathbb{R}^d$  and diffusion coefficient  $\sigma : \mathbb{R}^d \rightarrow \mathbb{R}^{d \times d}$ . The aim of this paper is to recover the latent representation  $f$  and the coefficients of the SDE that governs  $Z_t$  ( $\mu$  and  $\sigma$ ) from  $X_t$ .

We consider the following problem.

**Problem 1.** Find  $(\tilde{f}, \tilde{\mu}, \tilde{\sigma})$  such that (1) holds for  $\tilde{f}$ ,  $\tilde{\psi} = \tilde{f}^{-1}$ , and  $\{\tilde{Z}_t\}_{t \in \mathbb{T}}$  is a solution to the SDE with drift and diffusion coefficients  $\tilde{\mu}$  and  $\tilde{\sigma}$ , respectively.

Because the only available data is  $\{X_t\}_{t \in \mathbb{T}}$ , any solution of Problem 1 is a plausible description of the latent space. We now introduce the equivalence relation,

$$(f, \mu, \sigma) \sim (\tilde{f}, \tilde{\mu}, \tilde{\sigma}), \quad (5)$$

if there is an invertible function  $g : \mathbb{R}^d \rightarrow \mathbb{R}^d$  such that

- For any solution  $Y_t$  of (2),  $g(Y_t)$  is a solution to (2) with drift and diffusion coefficients  $\tilde{\mu}$  and  $\tilde{\sigma}$ , respectively<sup>1</sup>;
- $\tilde{f}(z) = (f \circ g^{-1})(z) \quad \forall z \in \mathbb{R}^d$ .

---

<sup>1</sup>An explicit formula for  $\tilde{\mu}$  and  $\tilde{\sigma}$ , depending on  $\mu$ ,  $\sigma$  and  $g$  can be obtained using Itô's Lemma [11].

This equivalence relation is very important for describing the solutions of Problem 1.

**Proposition 1.** *If  $(f, \mu, \sigma)$  is a solution to Problem 1 and  $(\tilde{f}, \tilde{\mu}, \tilde{\sigma}) \sim (f, \mu, \sigma)$ , then  $(\tilde{f}, \tilde{\mu}, \tilde{\sigma})$  is also a solution to Problem 1. In particular, we can only recover  $(f, \mu, \sigma)$  up to its equivalence class.*

*Proof.* If  $(f, \mu, \sigma) \sim (\tilde{f}, \tilde{\mu}, \tilde{\sigma})$ , then it exists an invertible function  $g$  such that  $\tilde{\mu}$  and  $\tilde{\sigma}$  are the drift and diffusion coefficients of the SDE that governs  $\tilde{Z}_t = g(Z_t)$ . We have  $\tilde{f} = f \circ g^{-1}$ , which implies

$$\tilde{f}(\tilde{Z}_t) = f(g^{-1}(g(Z_t))) = f(Z_t) = X_t,$$

and (1) holds for  $(\tilde{f}, \tilde{f}^{-1}, \tilde{Z}_t)$ , thus  $(\tilde{f}, \tilde{\mu}, \tilde{\sigma})$  is also a solution to Problem 1.  $\square$

Since we can only recover  $(f, \mu, \sigma)$  up to its equivalence class, we should focus on recovering an element of the equivalence which is easier to describe. The following result achieves that.

**Theorem 2.** *Suppose that  $(f, \mu, \sigma)$  is a solution to Problem 1, and that the following conditions are satisfied:*

- (i)  $\mu$  and  $\sigma$  are globally Lipschitz as in (4), and  $\sigma(y)$  is symmetric positive definite for all  $y \in \mathbb{R}^d$ .
- (ii)  $\sigma$  is differentiable everywhere and for all  $y \in \mathbb{R}^d$ .

$$\frac{\partial \sigma(y)}{\partial y_k} \sigma(y)^{-1} e_j = \frac{\partial \sigma(y)}{\partial y_j} \sigma(y)^{-1} e_k, \quad (6)$$

where  $e_j$  is the  $j$ -th canonical basis vector of  $\mathbb{R}^d$ .

Then there exists a solution  $(\tilde{f}, \tilde{\mu}, \tilde{\sigma})$  to Problem 1 such that  $\tilde{\sigma}(y) = I_d$  for all  $y \in \mathbb{R}^d$ , where  $I_d$  is the identity matrix of size  $d$ .

*Proof.* The crucial part of the proof is using Proposition 1 and finding an invertible function  $g$  such that  $g(Z_t)$  is governed by a SDE with an isotropic diffusion coefficient. This change of variable that reduces an SDE to one with isotropic diffusion is named Lamperti transform, and necessary and sufficient conditions for a SDE to be reducible and finding  $g$  are available in [12, Proposition 1]. The proof is completed by setting  $\tilde{f} = f \circ g^{-1}$ .  $\square$

Taking this result into consideration, we assume, for the rest of the paper, that  $\sigma(y) = I_d$  for all  $y \in \mathbb{R}^d$ , unless when specified otherwise.

## 5 Estimating the Latent SDE using a VAE

In this section we describe a method for recovering  $(f, \mu)$ , assuming an isotropic diffusion coefficient, using a VAE. While  $\{X_t\}_{t \in \mathbb{T}}$  is a stochastic process defined for all  $t \in \mathbb{T}$ , in practice, we sample  $X_t$  at discrete times and, for simplicity, we assume for most of the paper that the sampling frequency is constant. That is, we observe a time series  $\{X_t\}_{t \in \mathbf{T}}$ , where  $\mathbf{T} = \{i\Delta t, i \in \mathbb{N}, i \leq N\}$ , for some positive constant  $\Delta t$ .

In order to learn the decoder and the drift coefficient, we consider pairwise consecutive time series observations  $\mathbf{X} = (X_{t+\Delta t}, X_t)$ , which correspond to the latent variables  $\mathbf{Z} = (Z_{t+\Delta t}, Z_t)$ . Accordingly, we consider the following conditional generation model, with model parameters  $\theta = (f, \mu, \gamma)$ .

$$p_\theta(\mathbf{X}, \mathbf{Z}) = p_f(X_{t+\Delta t} | Z_{t+\Delta t}) p_\mu(Z_{t+\Delta t} | Z_t) p_f(X_t | Z_t) p_\gamma(Z_t), \quad (7)$$

where:

- The terms  $p_f(X_{t+\Delta t} | Z_{t+\Delta t})$  and  $p_f(X_t | Z_t)$  represent the mapping from latent to observed space, and are described by

$$p_f(X_t | Z_t) = p_\epsilon(X_t - f(Z_t)), \quad (8)$$

or equivalently,  $X_t = f(Z_t) + \epsilon$ , where  $\epsilon$  is a noise random variable independent from  $X_t$  and  $Z_t$ . In practice, we set  $\epsilon$  as a centered Gaussian random variable, with variance controlled by an hyperparameter.

- The prior distribution on the latent space is given by  $p_\gamma(Z_t)$ . This term is added to ease the training of the VAE.
- The term  $p_\mu(Z_{t+\Delta t}|Z_t)$  is related to the SDE dynamics. In order to model this equation with a conditional generation model, we use the Euler-Maruyama method. Recalling that  $Z_t$  is a solution to an SDE with an isotropic diffusion coefficient, and drift coefficient  $\mu : \mathbb{R}^d \rightarrow \mathbb{R}^d$ , we have

$$Z_{t+\Delta t} \approx Z_t + \mu(Z_t)\Delta t + W_{t+\Delta t} - W_t. \quad (9)$$

Since  $W_{t+\Delta t} - W_t$  is distributed as a multivariate centered Gaussian variable with variance  $\Delta t I_d$ , we define

$$p_\mu(Z_{t+\Delta t}|Z_t) = \frac{1}{\sqrt{2\pi\Delta t}^d} \exp\left(-\frac{\|Z_{t+\Delta t} - Z_t - \mu(Z_t)\Delta t\|^2}{2\Delta t}\right). \quad (10)$$

Followingly, we describe an encoder  $q(\mathbf{Z}|\mathbf{X})$ , that approximates the true posterior  $p_\theta(\mathbf{Z}|\mathbf{X})$ , which is computationally intractable. From (7), it follows that we can factorize

$$p_\theta(\mathbf{Z}|\mathbf{X}) = p_\theta(Z_{t+\Delta t}|X_{t+\Delta t}, Z_t)p_\theta(Z_t|X_t). \quad (11)$$

However, if  $\epsilon = 0$  in (8), since  $f$  is injective we would be able to determine  $Z_{t+\Delta t}$  from  $X_{t+\Delta t}$ . Although the noise  $\epsilon$  is not 0, we assume it is relatively small, and particularly is smaller than the noise related to the SDE term  $p_\mu(Z_{t+\Delta t}|Z_t)$ . Intuitively, that implies  $X_{t+\Delta t}$  gives much more information about  $Z_{t+\Delta t}$  than  $Z_t$ , and we can consider the approximation

$$p_\theta(Z_{t+\Delta t}|X_{t+\Delta t}, Z_t) \approx p_\theta(Z_{t+\Delta t}|X_{t+\Delta t}),$$

without losing too much information. This informal argument, which we formalize in technical appendix, motivates the decomposition of the encoder

$$q_\psi(\mathbf{Z}|\mathbf{X}) = q_\psi(Z_{t+\Delta t}|X_{t+\Delta t})q_\psi(Z_t|X_t). \quad (12)$$

This decomposition allows for using the same encoder twice, and therefore eases the training of the VAE. Let  $\mathcal{D} = \{x_{t+\Delta t}, x_t\}_{t \in \mathcal{T}}$  be the observed data, already paired into consecutive observations, and  $q_{\mathcal{D}}$  the empirical distribution in  $\mathcal{D}$ . We then train the VAE by minimizing the loss

$$\begin{aligned} \mathcal{L}(\theta, \psi) &:= \mathbb{E}_{q_{\mathcal{D}}(\mathbf{X})} [\mathbb{E}_{q_\psi(\mathbf{Z}|\mathbf{X})} [\log q_\psi(\mathbf{Z}|\mathbf{X}) - \log p_\theta(\mathbf{X}, \mathbf{Z})]], \\ &= D_{KL}(q_\psi(\mathbf{Z}|\mathbf{X})q_{\mathcal{D}}(\mathbf{X}) \parallel p_\theta(\mathbf{Z}|\mathbf{X})q_{\mathcal{D}}(\mathbf{X})) - \mathbb{E}_{q_{\mathcal{D}}(\mathbf{X})} [p_\theta(\mathbf{X})]. \end{aligned} \quad (13)$$

Here (13) can be thought of as the negative evidence lower bound; minimizing it forces  $q_\psi(\mathbf{Z}|\mathbf{X})$  to approximate  $p_\theta(\mathbf{Z}|\mathbf{X})$  while maximizing the likelihood of  $p_\theta(\mathbf{X})$  under the distribution  $q_{\mathcal{D}}$ . To calculate (13), we use the reparametrization trick [13] to backpropagate through the SDE, and the exact form of the KL divergence between two Gaussians which we describe in the technical appendix. The training algorithm then proceeds as a regular VAE.

## 6 Identifiability

In this section, we return to the topic of identifiability. Previously, we showed that we can assume that the diffusion coefficient is isotropic, and introduced the prior parameter  $\gamma$  as a mechanism to ease the training of the VAE. Here we provide identifiability results for the remaining model parameters  $\theta = (f, \mu, \gamma)$ .

A crucial element of our analysis is that the probability distribution of  $\mathbf{X} = (\hat{X}_{t+\Delta t}, \hat{X}_t)$  is defined by  $\theta$ , through equation (7), and any set of parameters  $\tilde{\theta} = (\tilde{f}, \tilde{\mu}, \tilde{\gamma})$  for which  $p_{\tilde{\theta}}(\mathbf{x})$  coincides with the true generative model  $p_{\theta^*}(\mathbf{x})$  of  $\mathbf{X}$  is a solution of Problem 1. When this happens, what is the relation between  $\theta$  and  $\theta^*$ ?

In the following theorem, we show that if the generative models coincide, then the corresponding parameters are equal up to an isometry. Recalling Proposition 1, it becomes clear why it is only possible to recover  $\theta$  up to an isometry: if  $g$  is an isometry and  $Z_t$  is a solution to an SDE with an isotropic diffusion coefficient, then  $g(Z_t)$  is a solution to another SDE with an isotropic diffusion coefficient.

**Theorem 3.** *Suppose that the true generative model of  $\mathbf{X}$  has parameters  $\theta^* = (f^*, \mu^*, \gamma^*)$ , and that the following technical conditions hold:*

1. *The set  $\{x \in \mathcal{X} | \psi_\epsilon(x) = 0\}$  has measure zero, where  $\psi_\epsilon$  is the characteristic function of the density  $p_\epsilon$  defined in (8).*
2.  *$f^*$  is injective and differentiable.*
3.  *$\mu^*$  is differentiable almost everywhere.*

*Then, for almost all values of  $\Delta t$ ,<sup>2</sup> if  $\theta = (f, \mu, \gamma)$  are other model parameters that yield the same generative distribution, that is*

$$p_\theta(x_{t+\Delta t}, x_t) = p_{\theta^*}(x_{t+\Delta t}, x_t) \quad \forall x_{t+\Delta t}, x_t \in \mathbb{R}^n, \quad (14)$$

*then  $\theta$  and  $\theta^*$  are equal up to an isometry. That is, there exists an orthogonal matrix  $Q$  and a vector  $b$ , such that for all  $z \in \mathbb{R}^d$ :*

$$f(z) = f^*(Qz + b), \quad (15)$$

$$\mu(z) = Q^T \mu^*(Qz + b), \quad (16)$$

*and*

$$p_\gamma(z) = p_{\gamma^*}(Qz + b). \quad (17)$$

The proof of Theorem 3 is closely related with the theory developed in [14], and is available in the technical appendix. Finally, we show the VAE framework presented in this paper can obtain the true model parameters in the limit of infinite data.

**Theorem 4.** *If  $p_\theta(\mathbf{Z}|\mathbf{X})$  can be approximated to arbitrary precision by  $q_\psi(\mathbf{Z}|\mathbf{X})$ , then, in the limit of infinite data, we obtain the true model parameters  $\theta^* = (f^*, \mu^*, \gamma^*)$ , up to an isometry, by minimizing the VAE loss (13) with respect both to  $\theta$  and  $\psi$ .*

*Proof.* See [14, Supplemental Material B.6]. □

## 7 Practical considerations

We made number of simplifying assumptions that may not hold in practical cases. Here we discuss some of their implications on the proposed method.

### 7.1 Time dependence and sampling frequency

In order to simplify the exposition of the results, we have considered SDE coefficients which are not time dependent, and assumed that the sampling frequency is fixed. However the proposed framework can also accommodate time dependent SDEs and variable sampling frequency with some modifications. A crucial fact is that even if  $\mu$  and  $\sigma$  are time-dependent, Theorem 2 also holds and we can still assume  $\sigma$  is isotropic. Then, to accommodate time dependent SDEs, we will need to modify the encoder and decoders to be time-dependent, that is, modify  $f$  and  $\psi$  to take the time  $t$  as another input. Finally, the drift coefficient will be also time-dependent; for two consecutive observations at times  $t_1$  and  $t_2$ , (9) becomes

$$Z_{t_2} \approx Z_{t_1} + \mu(Z_{t_1}, t_1)(t_2 - t_1) + W_{t_2} - W_{t_1}, \quad (18)$$

---

<sup>2</sup>That is, there is a finite set  $S$ , depending on  $\mu$ , such that if  $\Delta t \notin S$ , the condition holds.

and  $p_\mu(Z_{t_2}|Z_{t_1})$  is defined analogously to (10). We note however that this approach depends on the validity of approximation (18), and if this does not hold, for instance when  $t_2 - t_1$  is too large, an adjustment of the underlying integrator may be necessary, such as the one described in [15]. Finally, Theorems 3 and 4 also hold for this modifications. We provide further details on this topic in the technical appendix.

## 7.2 Determining the latent dimension

In order to learn the latent dimension, we suggest using the following architecture search procedure. Instead of considering an isotropic diffusion coefficient, we set  $\sigma(y) = D$  for all  $y \in \mathbb{R}^d$ , where  $D$  is a diagonal matrix with learnable diagonal entries. Starting with a guess for the latent dimension, we increase it if the image reconstruction is unsatisfactory, and decrease it if some of the diagonal entries of  $D$  are close to 0 (adding an  $\ell_1$  regularization to the diagonal entries of  $D$  will promote sparsity and help drive some of its values to 0).

In the technical appendix, we present an interpretability result that considers learnable diffusion coefficients. Unfortunately, this result requires conditions that do not apply for simpler SDEs, such as Brownian random walks, therefore we decided to present Theorem 3 instead.

# 8 Experiments

We consider 3 synthetic datasets to illustrate the efficacy of SDE-VAE. In all SDEs considered, the diffusion coefficient is the identity matrix, as suggested by Theorem 2.

## 8.1 Datasets

### 8.1.1 Stochastic Yellow Ball:

For this dataset, we simulate the stochastic motion of a yellow ball moving according to a given SDE using the Euler-Maruyama method. That is to say, the  $x$  and  $y$  coordinates of the center of the ball are governed by an SDE with an isotropic diffusion coefficient, and the drift coefficients are defined for  $(x, y) \in \mathbb{R}^2$  as follows.

$$\begin{aligned} \text{Constant: } \mu(x, y) &= (-1, 1); \\ \text{OU: } \mu(x, y) &= (-4x, -4y); \end{aligned}$$

The latent space dimension is 2, corresponding to the  $x$  and  $y$  coordinates of the ball. Figure 2 shows an example of the movement of the balls. We train the model on one realization of the SDE for 1000 time steps with  $\Delta t = 0.01$ . We rescale the realization of the SDE so that the  $x$  and  $y$  coordinates of the ball are always between 0 and 1; in practice, this only changes the map from latent to observed variables, and our method should still be able to recover the original latent SDE realization.

### 8.1.2 Stochastic Red Digits:

To further investigate the generative properties of the proposed method, we consider images of 2 digits from the MNIST dataset moving according to an SDE in the image plane, similarly to the dataset above, and use the Euler-Maruyama method to simulate the spatial positions of the two digits. In this case, the latent space is 4-dimensional, corresponding to the  $x$  and  $y$  coordinates of the center of each of the digits. Letting  $\mathbf{x} \in \mathbb{R}^2$  and  $\mathbf{y} \in \mathbb{R}^2$  be the  $x$  and  $y$  coordinates of each ball, then the drift coefficient is defined for  $(\mathbf{x}, \mathbf{y}) \in \mathbb{R}^4$  as follows.

$$\begin{aligned} \text{Constant: } \mu(\mathbf{x}, \mathbf{y}) &= (\mathbf{0}, \mathbf{0}); \\ \text{OU: } \mu(\mathbf{x}, \mathbf{y}) &= (-\mathbf{x} - 1, -\mathbf{y} + 1); \end{aligned}$$

Dataset	SDE	$\mathcal{L}_{\text{latent}}$	$\mathcal{L}_{\mu}$ MLP	$\mathcal{L}_{\mu}$ Parametric	$\mathcal{L}_{\mu}$ CRLB
Balls	Constant	$1.01(\pm 0.36)\times 10^{-1}$	$1.81(\pm 1.26)\times 10^0$	$6.82(\pm 2.54)\times 10^{-1}$	$2.00\times 10^{-1}$
	OU	$2.11(\pm 0.33)\times 10^{-2}$	$5.50(\pm 2.96)\times 10^{-1}$	$4.31(\pm 1.00)\times 10^{-1}$	$2.00\times 10^{-1}$
Digits	Constant	$7.05(\pm 2.81)\times 10^{-1}$	$7.05(\pm 7.03)\times 10^{-2}$	$3.41(\pm 4.19)\times 10^{-2}$	$4.00\times 10^{-2}$
	OU	$1.68(\pm 1.57)\times 10^{-1}$	$2.15(\pm 1.43)\times 10^{-1}$	$1.60(\pm 0.43)\times 10^{-1}$	$4.00\times 10^{-2}$
Wasserstein	OU	$6.65(\pm 4.06)\times 10^{-2}$	$3.69(\pm 4.06)\times 10^{-1}$	$6.96(\pm 9.39)\times 10^{-2}$	$1.00\times 10^{-1}$

Table 1: Comparison of the MSE defined in (19) for the proposed method across different datasets. The estimation error for the drift coefficient  $\mathcal{L}_{\mu}$  is reported for learning  $\mu$  with an MLP and a parametric form, and compared with the information theoretical Cramér Rao lower bound.

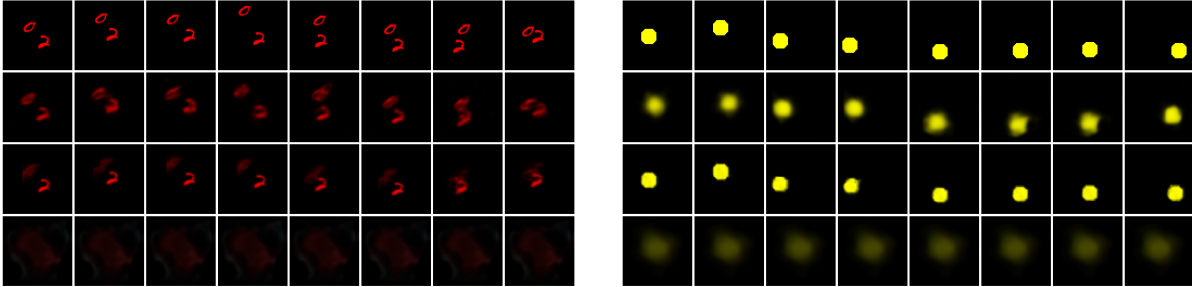


Figure 2: Comparison of image reconstruction for different autoencoders. The top row is the ground truth, second row is the proposed method, third row is DDPAE, and fourth row is ODE<sup>2</sup>VAE. Each sample is sampled every 8 time steps starting at  $t = 0$ .

Here,  $\mu(\mathbf{x}, \mathbf{y}) \in \mathbb{R}^4$  and the product of vectors is defined entry-wise. For each digit pair, we generate 10 trajectories of the SDE with 100 frames in each trajectory and  $\Delta t = 0.1$ . In this dataset, we also rescale the realization of the SDE so that the  $x$  and  $y$  coordinates of the digits are always between 0 and 1;

### 8.1.3 Wasserstein Interpolation:

Finally, we are interested in investigating the algorithm’s efficacy on a non movement dataset by generating a series of interpolations between two images according to their Wasserstein barycenters [16]. This experiment aims to consider the method’s performance on a more complicated dataset than the previous two. For instance, spatial position-based encodings of the objects in the images will not work in this case. An example of this dataset is in Figure 3 where we show interpolation between two images in the COIL 20 dataset [17]. We simulate a 1-D OU process with an isotropic diffusion coefficient which determines the relative weight of each image within the interpolation. The drift coefficient is defined as follows.

$$\text{OU: } \mu(x) = -2x \quad \forall x \in \mathbb{R}$$

We simulate 1000 images with  $\Delta t = 0.01$ . The realization of the SDE is rescaled so that the relative weight of each image is always between 0 and 1;

## 8.2 Experiment Setup

For all experiments, we use a convolutional encoder-decoder architecture. The latent drift coefficient  $\mu$  is represented as a multi layer perceptron (MLP). We consider the same network architectures between all experiments in order to maintain consistency. All architecture and hyper-parameter specifications are

Method	$\mathcal{L}_{\text{latent}}$ (affine)		Reconstruction error	
	Ball	Digits	Ball	Digits
Proposed	<b>2.19</b> ( $\pm 1.46$ ) $\times 10^{-2}$	<b>4.53</b> ( $\pm 1.78$ ) $\times 10^{-2}$	1.45( $\pm 8.81$ ) $\times 10^{-2}$	<b>3.14</b> ( $\pm 30.9$ ) $\times 10^{-3}$
DDPAE	8.12( $\pm 3.64$ ) $\times 10^{-2}$	3.77( $\pm 0.69$ ) $\times 10^{-1}$	<b>8.12</b> ( $\pm 71.0$ ) $\times 10^{-3}$	3.78( $\pm 43.6$ ) $\times 10^{-3}$
ODE <sup>2</sup> VAE	6.29( $\pm 2.25$ ) $\times 10^{-2}$	2.30( $\pm 0.60$ ) $\times 10^{-1}$	2.65( $\pm 13.8$ ) $\times 10^{-2}$	5.56( $\pm 54.1$ ) $\times 10^{-3}$

Table 2: Baseline comparison of the proposed method with DDPAE and ODE<sup>2</sup>VAE. The second and third columns compare the error for recovering the latent variables up to an affine map for the ball and digits dataset, while the last two columns compare the reconstruction error of each method for the same datasets.

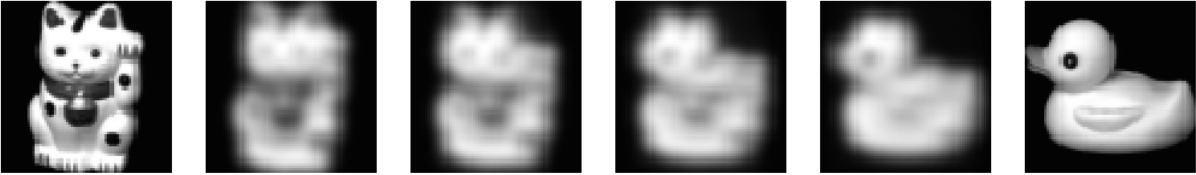


Figure 3: Example of interpolation between cat and duck images from the COIL 20 dataset, using the Wasserstein barycenters. Samples of the Wasserstein dataset are generated using this interpolation method, with relative weights governed by an SDE.

available in the technical appendix along with code to generate the datasets and run the algorithm and qualitative results. All image sizes are  $64 \times 64 \times 3$ .

We first test the proposed method on learning the latent SDEs in these datasets. In order to show evidence of the theoretical results presented in the Identifiability Section, we measure the mean square error (MSE) between the true latent representation and the representation obtained by the VAE, (up to an isometry) and compare the true drift coefficient  $\mu$  with the estimated one. Because Theorems 3 and 4 imply the true latent space and the one obtained by the VAE are related through an isometry, we measure the MSE using the following formulas.

$$\begin{aligned} \mathcal{L}_{\text{latent}} &= \frac{1}{N} \min_{Q,b} \sum_{t=0}^N \|Q\tilde{f}^{-1}(X_t) + b - Z_t\|_2^2, \\ \mathcal{L}_{\mu} &= \frac{1}{|\mathcal{X}|} \sum_{x \in \mathcal{X}} \|Q\hat{\mu}(Q^T(x-b), t) - \mu(x, t)\|_2^2. \end{aligned} \tag{19}$$

Here, the minimum is over all orthogonal matrices  $Q \in \mathbb{R}^{d \times d}$  and vectors  $b \in \mathbb{R}^d$ , and  $\tilde{f}^{-1}$  is the function learned by the VAE encoder. The minimizers admit a closed form solution which we describe in the technical appendix. We use the minimizers  $Q, b$  of  $\mathcal{L}_{\text{latent}}$  to calculate  $\mathcal{L}_{\mu}$ , and  $\mathcal{X}$  is the set of sampled points.  $\mathcal{X}$  is defined to be 50 points in each dimension, centered at  $\mathbf{a}$  and at most at  $\mathbf{s}$  distance from  $\mathbf{a}$ , where  $\mathbf{a}, \mathbf{s}$  are the average and standard deviation of  $Z_t$ .  $t$  is sampled over the time interval. All experiments with the proposed method are repeated with 5 independent runs, and the average and standard deviation are reported in Table 1. We also compare  $\mathcal{L}_{\mu}$  obtained by learning  $\mu$  using an MLP, with the error if we assume a parametric form for  $\mu$ , and a Cramér Rao lower bound (CRLB) for  $\mathcal{L}_{\mu}$ . The parametric form used for estimating  $\mu$  in these experiments is described in the technical appendix. The CRLB is obtained using an information theoretic argument, and provides a lower bound for the MSE of any estimator of  $\mu$ , therefore can be considered as a baseline of what is theoretically achievable. The derivation of the CRLB for these experiments is also described in the technical appendix.

We also compare the proposed method with two related methods, DDPAE [9] and ODE<sup>2</sup>VAE [6]. DDPAE uses a powerful recurrent neural network model to decompose the latent space into two components: one on content and one on position. This makes the position component related to our disentanglement and identification of the underlying SDE. The ODE<sup>2</sup>VAE model relies on latent ordinary differential equations (ODEs). While SDEs can be thought of as a stochastic generalization of ODEs, the ODE<sup>2</sup>VAE model is also able to deal with stochasticity. It is then fitting to compare the performance of the SDE based method and ODE<sup>2</sup>VAE.

In order to compare these methods to the proposed one, we consider the best affine transformation between the latent embeddings when the dimension is fixed, and compute the MSE between the transformed embeddings and the original SDE. To calculate the MSE for this experiment, we proceed similarly to (19), however we let  $Q$  be any square matrix in the optimization. The formula for calculating  $Q$  and  $b$  in this case is slightly different, and is also provided in the technical appendix. For this experiment, we compare with the best affine map, instead of orthogonal map (or isometry), since the scaling of the latent space of DDPAE and ODE<sup>2</sup>VAE can be much different than the true scale of the latent space (and therefore their latent space needs to be rescaled). For the ball and digits datasets, and OU process, we repeat this experiment for each method 5 times, and report the average and standard deviation in Table 2. These values should be comparable to the values reported in the third column of Table 1.

We additionally compare the MSE between the test data and its reconstruction, (encoding and decoding) using each of these methods, and report the results in Figure 2 and Table 2. The error is calculated over 100 images in a single run. We note that the comparison is primarily to confirm the reconstruction capabilities, but this does not represent the main points of learning the dynamics. Previous works [7,8] have compared the ability to learn the dynamics in videos by generating 100 runs, based on previous test frames, and reporting the one closer in MSE to the true rest of the video. However, given the high randomness/stochasticity of the datasets, 100 runs would not be enough to represent all possible future outcomes, and the results of that test would be highly affected by randomness.

Finally, we note that both baseline methods focus on spatial movements in their experiments and focus. DDPAE uses a decomposition in the latent space based on a spatial transformation, and ODE<sup>2</sup>VAE focuses on objects moving within the image plane in the empirical analysis. For these reasons, we opted to not compare these with the proposed method for the Wasserstein dataset.

### 8.3 Interpretation of results

Comparing  $\mathcal{L}_{\text{latent}}$  in Table 1 between the different experiments, we see that the proposed method is able to learn the latent representation better for the yellow ball, which was expected since this was the simplest dataset. Comparing  $\mathcal{L}_{\mu}$  with the theoretical CRLB, we observe that our method is able to recover the drift coefficient fairly well for the OU process in all datasets, and for the constant drift process (Brownian random walk) for the digits dataset, especially if  $\mu$  assumes a parametric form. On the other hand, we believe the performance for the yellow ball dataset, constant process, was hindered by the fact that any solution to that SDE is unbounded, and when we rescale the SDE, so that the coordinates are between 0 and 1, we lose information.

Comparing the three methods in Table 2, we observe the proposed method greatly outperforms the other methods in recovering the underlying latent dynamics. Regarding the reconstruction error, the proposed method is comparable with DPPAE, which uses a more complicated architecture, but we point out that the main focus of our work is to recover meaningful latent dynamics. We notice, both quantitatively in Table 2 and qualitatively in Figure 2, that the ODE<sup>2</sup>VAE method performs worse. While this method can handle stochasticity, it is outperformed by the other methods on these highly stochastic datasets.

## 9 Discussion

In this paper we present a novel approach to learn latent SDEs using VAEs. We also show that the presented method can recover the original latent map and the SDE coefficients up to an isometry. We finally provide

theoretical justification for the efficacy of the method.

However, there are a variety of additional avenues for expanding the method. Recently, the work by [18] describes an extension to the framework established by [14] wherein the authors propose a method that does not require knowledge of the intrinsic dimension. A similar approach can be employed in this method where eigenvalues of the estimated diffusion coefficient diminish to form a low rank matrix, indicating unnecessary components. Another extension would be to extend our results to diffusion coefficients that do not satisfy (6).

We can also consider alternative metrics rather than the KL divergence for regularizing the increments, such as the Fisher divergence. In other direction, a more thorough analysis of using a neural network to model the drift coefficient, versus parametric forms, or a dictionary of candidate functions, similar to [2], is warranted, in the interest of interpretability.

Finally, considering other types of stochastic processes, such as Lévy flights or jump processes, could provide additional meaningful avenues for applications of the work.

## Acknowledgment

This work was supported in part by Office of Naval Research Grant No. N00014-18-1-2244. AH was partly supported by the National Science Foundation Graduate Research Fellowship.

## References

- [1] Stefano M Iacus. *Simulation and inference for stochastic differential equations: with R examples*. Springer Science & Business Media, 2009.
- [2] Samuel H Rudy, Steven L Brunton, Joshua L Proctor, and J Nathan Kutz. Data-driven discovery of partial differential equations. *Science Advances*, 3(4):e1602614, 2017.
- [3] Lorenzo Boninsegna, Feliks Nüske, and Cecilia Clementi. Sparse learning of stochastic dynamical equations. *The Journal of chemical physics*, 148(24):241723, 2018.
- [4] Xuechen Li, Ting-Kam Leonard Wong, Ricky TQ Chen, and David Duvenaud. Scalable gradients for stochastic differential equations. *arXiv preprint arXiv:2001.01328*, 2020.
- [5] Lea Duncker, Gergo Bohner, Julien Boussard, and Maneesh Sahani. Learning interpretable continuous-time models of latent stochastic dynamical systems. In *International Conference on Machine Learning*, pages 1726–1734, 2019.
- [6] Cagatay Yildiz, Markus Heinonen, and Harri Lahdesmaki. ODE2VAE: Deep generative second order ODEs with Bayesian neural networks. In *Advances in Neural Information Processing Systems*, pages 13412–13421, 2019.
- [7] Mohammad Babaeizadeh, Chelsea Finn, Dumitru Erhan, Roy H. Campbell, and Sergey Levine. Stochastic variational video prediction. In *International Conference on Learning Representations*, 2018.
- [8] Manoj Kumar, Mohammad Babaeizadeh, Dumitru Erhan, Chelsea Finn, Sergey Levine, Laurent Dinh, and Durk Kingma. Videoflow: A conditional flow-based model for stochastic video generation. In *International Conference on Learning Representations*, 2020.
- [9] Jun-Ting Hsieh, Bingbin Liu, De-An Huang, Li F Fei-Fei, and Juan Carlos Niebles. Learning to decompose and disentangle representations for video prediction. In *Advances in Neural Information Processing Systems*, pages 517–526, 2018.
- [10] Bernt Øksendal. Stochastic differential equations. In *Stochastic differential equations*, pages 65–84. Springer, 2003.

- [11] Hiroshi Kunita and Shinzo Watanabe. On square integrable martingales. *Nagoya Mathematical Journal*, 30:209–245, 1967.
- [12] Yacine Aït-Sahalia. Closed-form likelihood expansions for multivariate diffusions. *The Annals of Statistics*, 36(2):906–937, 2008.
- [13] Diederik P Kingma and Max Welling. Auto-encoding variational Bayes. *arXiv preprint arXiv:1312.6114*, 2013.
- [14] Ilyes Khemakhem, Diederik P Kingma, and Aapo Hyvärinen. Variational autoencoders and nonlinear ICA: A unifying framework. *arXiv preprint arXiv:1907.04809*, 2019.
- [15] SC Kou, Benjamin P Olding, Martin Lysy, and Jun S Liu. A multiresolution method for parameter estimation of diffusion processes. *Journal of the American Statistical Association*, 107(500):1558–1574, 2012.
- [16] Justin Solomon, Fernando De Goes, Gabriel Peyré, Marco Cuturi, Adrian Butscher, Andy Nguyen, Tao Du, and Leonidas Guibas. Convolutional wasserstein distances: Efficient optimal transportation on geometric domains. *ACM Transactions on Graphics (TOG)*, 34(4):1–11, 2015.
- [17] Sameer A Nene, Shree K Nayar, Hiroshi Murase, et al. Columbia object image library (coil-20). 1996.
- [18] Peter Sorrenson, Carsten Rother, and Ullrich Köthe. Disentanglement by nonlinear ICA with general incompressible-flow networks (GIN). *arXiv preprint arXiv:2001.04872*, 2020.
- [19] John M Lee. Smooth manifolds. In *Introduction to Smooth Manifolds*. Springer, 2013.
- [20] John C Gower, Garnt B Dijkstra, et al. *Procrustes problems*, volume 30. Oxford University Press on Demand, 2004.
- [21] Ilya Tolstikhin, Olivier Bousquet, Sylvain Gelly, and Bernhard Schoelkopf. Wasserstein auto-encoders. *arXiv preprint arXiv:1711.01558*, 2017.

The technical appendix is organized as follows. In Appendix A, we explain in greater detail some aspects of the proposed variational auto-encoder (VAE) model, and in Appendix B, we prove Theorem 3. In Appendix C, we present further details on the aspects raised in the Practical Considerations Section of the main submission. Followingly, in Appendix D we show how we calculate (19) and in Appendix E we show how we obtained the Cramér Rao lower bound presented in the main submission. Finally, in Appendix F we go over technical details in the experiments, such as the architecture and hyper-parameters used, and including the parametric form assumed for the drift coefficient, which correspond to the results reported in the second to last column of Table 1.

## A. Notes on the VAE loss

Here we go into detail on various aspects of the VAE loss (13). Particularly, we justify the decomposition (12) and explain how we calculate the loss (13) during training.

### A.1 Encoder decomposition

Here we further justify (12). To that end, we use the notion of mutual information. Informally, the mutual information measures the information in common between two random variables, or equivalently, how much information is obtained about one of the variables by observing the other. Formally, the mutual information between the random variables  $X$  and  $Y$ , with joint distribution  $p_{X,Y}$ , marginal distributions  $p_X$  and  $p_Y$ , respectively, and conditional distribution  $p_{Y|X}$ , is defined as:

$$\begin{aligned} I(X;Y) &:= D_{KL}(p_{X,Y}(X,Y) \parallel p_X(X)p_Y(Y)), \\ &= \mathbb{E}_{p_X(X)} [D_{KL}(p_{Y|X}(Y|X) \parallel p_Y(Y))]. \end{aligned} \tag{A.1}$$

We study the mutual information between  $Z_{t+\Delta t}$  and the joint distribution of  $(X_{t+\Delta t}, Z_t)$ . On one hand, this measures the amount of information one gets from  $Z_{t+\Delta t}$  by observing all of  $X_{t+\Delta t}, Z_t$ . On the other hand, the term  $p(Z_t|X_{t+\Delta t}, Z_t)$  both appears in the definition of  $I(Z_{t+\Delta t}; X_{t+\Delta t}, Z_t)$  and in the Kullback-Leibler (KL) divergence term in (13). Moreover, we compare  $I(Z_{t+\Delta t}; X_{t+\Delta t}, Z_t)$  with  $I(Z_{t+\Delta t}; X_{t+\Delta t})$ , in order to justify the approximation  $p(Z_t|X_{t+\Delta t}, Z_t) \approx p(Z_t|X_{t+\Delta t})$ . Our assumption is that the variance of  $\epsilon$  in (8) is much smaller than the variance of  $W_{t+\Delta t} - W_t$  in (9), which implies that  $I(Z_{t+\Delta t}; X_{t+\Delta t}) \gg I(Z_{t+\Delta t}; Z_t)$ . By the chain rule of mutual information, the following identities hold:

$$\begin{aligned} I(Z_{t+\Delta t}; X_{t+\Delta t}, Z_t) &= I(Z_{t+\Delta t}; X_{t+\Delta t}) + I(Z_{t+\Delta t}; Z_t|X_{t+\Delta t}), \\ &= I(Z_{t+\Delta t}; X_{t+\Delta t}) + I(Z_{t+\Delta t}, X_{t+\Delta t}; Z_t) - I(X_{t+\Delta t}; Z_t), \\ &\leq I(Z_{t+\Delta t}; X_{t+\Delta t}) + I(Z_{t+\Delta t}, X_{t+\Delta t}; Z_t). \end{aligned} \tag{A.2}$$

Note that (7) implies that  $X_{t+\Delta t}$  and  $Z_t$  are conditionally independent given  $Z_{t+\Delta t}$ , which implies that  $I(X_{t+\Delta t}; Z_t|Z_{t+\Delta t}) = 0$  and, applying the chain rule again,  $I(Z_{t+\Delta t}, X_{t+\Delta t}; Z_t) = I(Z_{t+\Delta t}; Z_t)$ . Therefore (A.2) is equivalent to:

$$I(Z_{t+\Delta t}; X_{t+\Delta t}, Z_t) \leq I(Z_{t+\Delta t}; X_{t+\Delta t}) + I(Z_{t+\Delta t}; Z_t). \tag{A.3}$$

The argument is now justified by our assumption that  $I(Z_{t+\Delta t}; Z_t) \ll I(Z_{t+\Delta t}; X_{t+\Delta t})$ .

### A.2 Calculating the VAE loss

Here, we explain how we calculate the expectation in (13). We use three techniques: Exact formula (when possible), the reparametrization trick [13] and a first order Taylor approximation, which we explain as follows. Let  $Z$  be a random variable with expectation  $\mu$ , and suppose we want to estimate  $\mathbb{E}[f(Z)]$  for some function  $f$ . On one hand, we can use the reparametrization trick to estimate this, but an even simpler way is the

rough estimate  $\mathbb{E}[f(Z)] \approx f(\mu)$ . This corresponds to the exact value of a first order Taylor approximation of  $f$ :

$$\begin{aligned}\mathbb{E}[f(Z)] &= \mathbb{E} [f(\mu) + J_f(\mu)(Z - \mu) + \{2^{\text{nd}} \text{ order and higher terms}\}], \\ &= f(\mu) + \{2^{\text{nd}} \text{ order and higher terms}\}.\end{aligned}$$

Getting back to (13), expanding it we get

$$\mathcal{L}(\theta, \psi) = \mathbb{E}_{q_{\mathcal{D}}(\mathbf{X})} [\mathbb{E}_{q_{\psi}(\mathbf{Z}|\mathbf{X})} [\log q_{\psi}(Z_{t+\Delta t}|X_{t+\Delta t}) + \log q_{\psi}(Z_t|X_t) \tag{A.4}$$

$$- \log p_{\mu}(Z_{t+\Delta t}|Z_t) - \log p_{\gamma}(Z_t) \tag{A.5}$$

$$- \log p_f(X_{t+\Delta t}|Z_{t+\Delta t}) - \log p_f(X_t|Z_t)] \tag{A.6}$$

We now explain how we calculate/estimate each of the expectations (A.4), (A.5) and (A.6). As in most VAE's, our encoder  $q_{\psi}$  is given by a Gaussian distribution conditioned on  $X_t$ . We define  $\boldsymbol{\mu}_q(X_t)$  and  $\mathbf{L}_q(X_t)$  as the neural networks that encode its mean and its Cholesky decomposition of the covariance<sup>3</sup>, respectively, getting:

$$q_{\psi}(Z_t|X_t) = \frac{1}{\sqrt{2\pi}^d |\det \mathbf{L}_q(X_t)|} \exp\left(-\frac{\|\mathbf{L}_q(X_t)^{-1}(Z_t - \boldsymbol{\mu}_q(X_t))\|^2}{2}\right).$$

This implies  $\mathbb{E}[Z_t|X_t] = \boldsymbol{\mu}_q(X_t)$  and  $\mathbb{E}[Z_t Z_t^T|X_t] = \mathbf{L}_q(X_t)\mathbf{L}_q(X_t)^T + \boldsymbol{\mu}_q(X_t)\boldsymbol{\mu}_q(X_t)^T$ , thus (A.4) can be calculated exactly:<sup>4</sup>

$$\begin{aligned}\mathbb{E}_{q_{\psi}(\mathbf{Z}|\mathbf{X})} [\log q_{\psi}(Z_{t+\Delta t}|X_{t+\Delta t})] \\ &= -\log |\det \mathbf{L}_q(X_t)| - \frac{1}{2} \mathbb{E} [\text{tr} (\mathbf{L}_q(X_t)^{-T} \mathbf{L}_q(X_t)^{-1} (Z_t - \boldsymbol{\mu}_q(X_t))(Z_t - \boldsymbol{\mu}_q(X_t))^T)], \\ &= -\log |\det \mathbf{L}_q(X_t)| - \frac{1}{2} \mathbb{E} [\text{tr} (\mathbf{L}_q(X_t)^{-T} \mathbf{L}_q(X_t)^{-1} \mathbf{L}_q(X_t) \mathbf{L}_q(X_t)^T)], \\ &= -\log |\det \mathbf{L}_q(X_t)| - \frac{d}{2}.\end{aligned}$$

While training, we observed the best prior distribution  $\gamma$  was either a Gaussian distribution with a high variance, or even an uniform distribution, and for both these cases the expectation can be calculated exactly. The other term in (A.5) is equal to:

$$\begin{aligned}\mathbb{E}_{q_{\psi}(\mathbf{Z}|\mathbf{X})} [-\log p_{\mu}(Z_{t+\Delta t}|Z_t)] \\ &= \frac{d}{2} \log \Delta t + \frac{1}{2\Delta t} \mathbb{E} \left[ \text{tr} \left( (Z_{t+\Delta t} - Z_t - \mu(Z_t)\Delta t)(Z_{t+\Delta t} - Z_t - \mu(Z_t)\Delta t)^T \right) \right].\end{aligned}$$

We note that the only expectations that cannot be calculated exactly are the ones involving  $\mu(Z_t)$ , thus we use the first order approximation  $\mu(Z_t) \approx \mu(\boldsymbol{\mu}_q(X_t))$ . Calculating the other expectations, and noting that the definition  $q_{\psi}(\mathbf{Z}|\mathbf{X})$  implies that  $\text{Cov}(Z_t, Z_{t+\Delta t}) = 0$ , we get the formula:

$$\begin{aligned}\mathbb{E}_{q_{\psi}(\mathbf{Z}|\mathbf{X})} [-\log p_{\mu}(Z_{t+\Delta t}|Z_t)] \\ &= \frac{d}{2} \log \Delta t + \frac{1}{2\Delta t} \text{tr}(\mathbf{L}_q(X_t)\mathbf{L}_q(X_t)^T) + \frac{1}{2\Delta t} \text{tr}(\mathbf{L}_q(X_{t+\Delta t})\mathbf{L}_q(X_{t+\Delta t})^T) \\ &\quad + \frac{1}{2\Delta t} \|\boldsymbol{\mu}_q(X_{t+\Delta t}) - \boldsymbol{\mu}_q(X_t) - \mu(\boldsymbol{\mu}_q(X_t))\|^2.\end{aligned}$$

Finally we model the noise  $\epsilon$  in (A.6) as a centered Gaussian random variable with variance  $\epsilon I$ , where  $\epsilon$  is a fixed hyper-parameter. We have,

$$\mathbb{E}_{q_{\psi}(\mathbf{Z}|\mathbf{X})} [-\log p_f(X_t|Z_t)] = \frac{d}{2} \log \epsilon + \frac{1}{2\epsilon} \mathbb{E} [\|f(Z_t) - X_t\|^2],$$

and use the reparametrization trick to calculate this.

<sup>3</sup>That is,  $\Sigma(X_t) = \mathbf{L}_q(X_t)\mathbf{L}_q(X_t)^T$

<sup>4</sup>We disregard the term  $\sqrt{2\pi}^d$  since this term is not needed in the optimization.

## B. Proof of Theorem 3

Our proof is very similar to the proof of [14, Theorem 1]. However, we cannot use that result directly, since our generation model is slightly different. Therefore we replicate the proof here, applied to our generation model, but suggest consulting [14] to understand more intricate details of the proof.

Our proof is split in 3 steps:

- (I) First, we write our generation model as a convolution that depends on the noise  $\epsilon$ , to reduce the equality  $p_\theta(\mathbf{x}) = p_{\theta^*}(\mathbf{x})$  to the noiseless case, obtaining (B.1).
- (II) Next, we use some algebraic tricks to get a linear dependence between  $f_*^{-1}$  and  $f^{-1}$ , obtaining (B.1)-(B.13)
- (III) Finally, we keep using algebraic manipulations to get the rest of the statements in the theorem.

### Step (I)

Let  $\mathcal{Z} = \mathbb{R}^d$  be the latent space,  $\mathcal{X} = f(\mathcal{Z})$ , that is,  $x \in \mathcal{X}$  if there is  $z \in \mathcal{Z}$  such that  $f(z) = x$ . First, we write  $p_\theta(x_{t+\Delta t}, x_t)$  as a convolution.

$$\begin{aligned} p_\theta(x_{t+\Delta t}, x_t) &= \int_{\mathcal{Z}} \int_{\mathcal{Z}} p_\epsilon(x_{t+\Delta t} - f(z_{t+\Delta t})) p_\epsilon(x_t - f(z_t)) q_{\mu, \gamma}(z_{t+\Delta t}, z_t) dz_{t+\Delta t} dz_t, \end{aligned} \quad (\text{i})$$

$$= \int_{\mathcal{X}} \int_{\mathcal{X}} p_\epsilon(x_{t+\Delta t} - \tilde{x}_{t+\Delta t}) p_\epsilon(x_t - \tilde{x}_t) q_{\mu, \gamma, f^{-1}}(\tilde{x}_{t+\Delta t}, \tilde{x}_t) d\tilde{x}_{t+\Delta t} d\tilde{x}_t, \quad (\text{ii})$$

$$= \int_{\mathbb{R}^n} \int_{\mathbb{R}^n} p_\epsilon(x_{t+\Delta t} - \tilde{x}_{t+\Delta t}) p_\epsilon(x_t - \tilde{x}_t) q_{\mu, \gamma, f^{-1}, \mathcal{X}}(\tilde{x}_{t+\Delta t}, \tilde{x}_t) d\tilde{x}_{t+\Delta t} d\tilde{x}_t, \quad (\text{iii})$$

$$= [(p_\epsilon \times p_\epsilon) * q_{\mu, \gamma, f^{-1}, \mathcal{X}}](\tilde{x}_{t+\Delta t}, \tilde{x}_t), \quad (\text{iv})$$

where in:

- (i) We write  $p_\theta(x_{t+\Delta t}, x_t)$  as the integration over  $z_t, z_{t+\Delta t}$  of  $p_\theta(x_{t+\Delta t}, x_t, z_{t+\Delta t}, z_t)$ , expand  $p_\theta$  as in (7), and let

$$q_{\mu, \gamma}(z_{t+\Delta t}, z_t) = p_\mu(z_{t+\Delta t} | z_t) p_\gamma(z_t).$$

- (ii) We do the change of variable  $\tilde{x}_t = f(z_t)$  and similarly for  $\tilde{x}_{t+\Delta t}$ . As in [14], the change of variable volume term for  $\tilde{x}_t$  is

$$\text{vol } J_{f^{-1}}(\tilde{x}_t) := \sqrt{\det(J_f(f^{-1}(\tilde{x}_t))^T J_f(f^{-1}(\tilde{x}_t)))},$$

and  $\tilde{x}_{t+\Delta t}$  is analogous. We then let

$$q_{\mu, \gamma, f^{-1}}(\tilde{x}_{t+\Delta t}, \tilde{x}_t) = \text{vol } J_{f^{-1}}(\tilde{x}_t) \text{vol } J_{f^{-1}}(\tilde{x}_{t+\Delta t}) q_{\mu, \gamma}(f^{-1}(\tilde{x}_{t+\Delta t}), f^{-1}(\tilde{x}_t)).$$

- (iii) We let

$$q_{\mu, \gamma, f^{-1}, \mathcal{X}}(\tilde{x}_{t+\Delta t}, \tilde{x}_t) = \mathbb{1}_{\mathcal{X}}(\tilde{x}_{t+\Delta t}) \mathbb{1}_{\mathcal{X}}(\tilde{x}_t) q_{\mu, \gamma, f^{-1}}(\tilde{x}_{t+\Delta t}, \tilde{x}_t),$$

so that the domain of the integral may be  $\mathbb{R}^n$  instead of  $\mathcal{X}$ .

- (iv) We finally notice the convolution formula, with  $(p_\epsilon \times p_\epsilon)(\tilde{x}_{t+\Delta t}, \tilde{x}_t) = p_\epsilon(\tilde{x}_{t+\Delta t}) p_\epsilon(\tilde{x}_t)$ .

We now have that if  $p_\theta(x_{t+\Delta t}, x_t) = p_{\theta^*}(x_{t+\Delta t}, x_t)$  for all  $x_{t+\Delta t}, x_t \in \mathbb{R}^n$ , then by taking the Fourier transform we get that for all  $x_{t+\Delta t}, x_t \in \mathbb{R}^n$  (or  $\omega_{t+\Delta t}, \omega_t \in \mathbb{R}^n$  when applicable)

$$\begin{aligned} [(p_\epsilon \times p_\epsilon) * q_{\mu, \gamma, f^{-1}, \mathcal{X}}](x_{t+\Delta t}, x_t) &= [(p_\epsilon \times p_\epsilon) * q_{\mu_*, \gamma_*, f_*^{-1}, \mathcal{X}_*}](x_{t+\Delta t}, x_t), \\ \mathcal{F}q_{\mu, \gamma, f^{-1}, \mathcal{X}}(\omega_{t+\Delta t}, \omega_t)\psi_\epsilon(\omega_{t+\Delta t})\psi_\epsilon(\omega_t) &= \mathcal{F}q_{\mu_*, \gamma_*, f_*^{-1}, \mathcal{X}_*}(\omega_{t+\Delta t}, \omega_t)\psi_\epsilon(\omega_{t+\Delta t})\psi_\epsilon(\omega_t), \\ \mathcal{F}q_{\mu, \gamma, f^{-1}, \mathcal{X}}(\omega_{t+\Delta t}, \omega_t) &= \mathcal{F}q_{\mu_*, \gamma_*, f_*^{-1}, \mathcal{X}_*}(\omega_{t+\Delta t}, \omega_t), \\ q_{\mu, \gamma, f^{-1}, \mathcal{X}}(x_{t+\Delta t}, x_t) &= q_{\mu_*, \gamma_*, f_*^{-1}, \mathcal{X}_*}(x_{t+\Delta t}, x_t), \end{aligned}$$

where  $\mathcal{F}$  denotes Fourier Transform and  $\psi_\epsilon = \mathcal{F}p_\epsilon$  is the characteristic function of  $\epsilon$ . Here condition 1 guarantees that we can divide by  $\psi_\epsilon(\omega_{t+\Delta t})\psi_\epsilon(\omega_t)$ . This equality for all  $x_t, x_{t+\Delta t}$  implies that  $\mathcal{X} = f(\mathcal{Z}) = f^*(\mathcal{Z}) = \mathcal{X}^*$  and, for all  $x_t, x_{t+\Delta t}$  in  $\mathcal{X}$ ,

$$\begin{aligned} \log \text{vol } J_{f_*^{-1}}(x_{t+\Delta t}) + \log \text{vol } J_{f_*^{-1}}(x_t) + \log p_{\mu_*}(f_*^{-1}(x_{t+\Delta t})|f_*^{-1}(x_t)) + \log p_{\gamma_*}(f_*^{-1}(x_t)) \\ = \log \text{vol } J_{f^{-1}}(x_{t+\Delta t}) + \log \text{vol } J_{f^{-1}}(x_t) + \log p_\mu(f^{-1}(x_{t+\Delta t})|f^{-1}(x_t)) + \log p_\gamma(f^{-1}(x_t)). \end{aligned} \quad (\text{B.1})$$

## Step (II)

We have

$$\log p_\mu(f^{-1}(x_{t+\Delta t})|f^{-1}(x_t)) = -\frac{\|f^{-1}(x_{t+\Delta t}) - f^{-1}(x_t) - \mu(f^{-1}(x_t))\Delta t\|^2}{2\Delta t}.$$

Let

$$\lambda(x_t) = f^{-1}(x_t) - \mu(f^{-1}(x_t))\Delta t, \quad (\text{B.2})$$

$$\psi(x_t) = \text{vol } J_{f^{-1}}(x_t) + \log p_\gamma(f^{-1}(x_t)) - \frac{\|\lambda(x_t)\|^2}{2\Delta t}, \quad (\text{B.3})$$

and

$$\varphi(x_{t+\Delta t}) = \text{vol } J_{f^{-1}}(x_{t+\Delta t}) - \frac{\|f^{-1}(x_{t+\Delta t})\|^2}{2\Delta t}, \quad (\text{B.4})$$

and define analogously  $\lambda_*, \psi_*$  and  $\varphi_*$ . We have for all  $x_t, x_{t+\Delta t}$  in  $\mathcal{X}$ ,

$$\psi(x_t) + \frac{1}{\Delta t} \langle f^{-1}(x_{t+\Delta t}), \lambda(x_t) \rangle + \varphi(x_{t+\Delta t}) = \psi_*(x_t) + \frac{1}{\Delta t} \langle f_*^{-1}(x_{t+\Delta t}), \lambda_*(x_t) \rangle + \varphi_*(x_{t+\Delta t}). \quad (\text{B.5})$$

Let  $w_0$  be some element in  $\mathcal{X}$ , then subtracting two equations we obtain

$$\langle f^{-1}(x_{t+\Delta t}), \lambda(x_t) - \lambda(w_0) \rangle + \zeta(x_t) - \zeta(w_0) = \langle f_*^{-1}(x_{t+\Delta t}), \lambda_*(x_t) - \lambda_*(w_0) \rangle, \quad (\text{B.6})$$

where  $\zeta(x) = (\psi(x_t) - \psi_*(x_t))\Delta t$ . Let  $z_0 = f_*^{-1}(w_0)$  and  $z_1, \dots, z_d$  a set of vectors in  $\mathcal{Z}$  such that  $z_1 - z_0, \dots, z_d - z_0$  are linearly independent. Let  $\mathbf{Z}$  the  $d \times d$  matrix such that its  $i$ -th column is  $z_i - z_0$  (by the hypothesis,  $\mathbf{Z}$  is an invertible matrix). Moreover let  $\mathbf{M}_*$  the  $d \times d$  matrix with  $i$ -th column defined by  $\mathbf{M}_i = \mu_*(z_i) - \mu_*(z_0)$ , and finally let  $\mathbf{\Lambda}_*$  be the matrix with  $i$ -th column defined by  $\mathbf{\Lambda}_{*i} = \lambda_*(f_*(z_i)) - \lambda_*(w_0)$ . By construction we have  $\mathbf{\Lambda}_* = \mathbf{Z} - \Delta t \mathbf{M}_*$ , or equivalently

$$\mathbf{\Lambda}_* \mathbf{Z}^{-1} = I - \Delta t \mathbf{M}_* \mathbf{Z}^{-1}. \quad (\text{B.7})$$

Therefore  $\mathbf{\Lambda} \mathbf{Z}^{-1}$  is singular only if  $\frac{1}{\Delta t}$  is an eigenvalue of  $\mathbf{M}_* \mathbf{Z}^{-1}$ . Since that set of eigenvalues is finite, we set  $S$  in the theorem statement to be

$$S = \left\{ \lambda : \frac{1}{\lambda} \text{ is a positive eigenvalue of } \mathbf{M}_* \mathbf{Z}^{-1} \right\} \quad (\text{B.8})$$

If now  $\Delta t \in \mathbb{R}^+ \setminus S$ , the matrix  $\mathbf{\Lambda}_* \mathbf{Z}^{-1}$  is non-singular, which implies  $\mathbf{\Lambda}_*$  is non-singular. Let  $\mathbf{\Lambda}_*$  defined as above, define  $\mathbf{\Lambda}$  analogously for  $\lambda$ , and let  $\psi \in \mathbb{R}^d$  such that

$$\psi_i = \zeta(f_*(z_i)) - \zeta(w_0).$$

We write (B.6) in matrix notation for  $x_t = f(z_0), \dots, f(z_d)$ .

$$\mathbf{\Lambda}_*^T f_*^{-1}(x_{t+\Delta t}) = \mathbf{\Lambda}^T f^{-1}(x_{t+\Delta t}) + \boldsymbol{\psi}, \quad (\text{B.9})$$

which implies that

$$f_*^{-1}(x_{t+\Delta t}) = \mathbf{\Lambda}_*^{-T} \mathbf{\Lambda}^T f^{-1}(x_{t+\Delta t}) + \mathbf{\Lambda}_*^{-T} \boldsymbol{\psi}, \quad (\text{B.10})$$

holds for all  $x_{t+\Delta t} \in \mathcal{X}$ . Equivalently, for all  $z \in \mathcal{Z}$ ,  $f_*(z) \in \mathcal{X}$  and

$$z = \mathbf{\Lambda}_*^{-T} \mathbf{\Lambda}^T f^{-1}(f_*(z)) + \mathbf{\Lambda}_*^{-T} \boldsymbol{\psi}, \quad (\text{B.11})$$

If we take the derivatives on  $z$  on both sides, we get

$$I = \mathbf{\Lambda}_*^{-T} \mathbf{\Lambda}^T J_{f^{-1} \circ f_*}(z). \quad (\text{B.12})$$

Since the matrix  $I$  is non-singular, this implies  $\mathbf{\Lambda}_*^{-T} \mathbf{\Lambda}^T$  is a non-singular matrix. Therefore there exists an invertible matrix  $Q$  and a vector  $b$  such that

$$f_*^{-1}(x_{t+\Delta t}) = Q f^{-1}(x_{t+\Delta t}) + b. \quad (\text{B.13})$$

### Step (III)

Equation (B.13) implies that for all  $z \in \mathcal{Z}$

$$\begin{aligned} f(z) &= f_*(f_*^{-1}(f(z))), \\ &= f_*(Q f^{-1}(f(z)) + b), \\ &= f_*(Qz + b). \end{aligned}$$

Moreover  $J_f = J_{f_*} Q$ , and  $\log \text{vol } J_{f^{-1}} = \log \text{vol } J_{f_*^{-1}} + \log |\det Q|$ . Now replacing  $x_{t+\Delta t}$  by  $f(z)$  on (B.5) and using (B.13) and (B.3), we get for all  $z \in \mathcal{Z}$  and  $x_t \in \mathcal{X}$ ,

$$\psi(x_t) + \frac{1}{\Delta t} \langle z, \lambda(x_t) \rangle - \frac{\|z\|^2}{2\Delta t} + \log |\det Q| = \psi_*(x_t) + \frac{1}{\Delta t} \langle Qz + b, \lambda_*(x_t) \rangle - \frac{\|Qz + b\|^2}{2\Delta t}. \quad (\text{B.14})$$

Taking derivatives with respect to  $z$ , we get

$$\lambda(x_t) - z = Q^T \lambda_*(x_t) - Q^T Qz - Q^T b. \quad (\text{B.15})$$

Taking derivatives again we get  $Q^T Q = I$ , thus  $Q$  is orthogonal. Replacing this back in (B.15), we get

$$\lambda_*(x_t) = Q \lambda(x_t) + b. \quad (\text{B.16})$$

Replacing (B.2), letting  $f(z) = x_t$  and using (B.13), we get for all  $z \in \mathcal{Z}$ ,

$$Qz + b - \mu_*(Qz + b)\Delta t = Qz - Q\mu(z)\Delta t + b, \quad (\text{B.17})$$

which implies  $\mu(z) = Q^T \mu_*(Qz + b)$  for all  $z \in \mathcal{Z}$ . Finally, replacing all equations obtained in (B.14), and using (B.3) and  $|\det Q| = 1$  (since  $Q$  is orthogonal), we get

$$\log p_\gamma(f^{-1}(x_t)) = \log p_{\gamma_*}(f_*^{-1}(x_t)), \quad (\text{B.18})$$

and (17) follows from taking  $x_t = f(z)$  and using (B.13).  $\square$

## C. Supplementary results regarding practical considerations

Here we complement present the proof of several results presented in the main submission.

## C.1 On Time-dependent SDEs

On the main submission, we focused on time-independent SDEs, however also mention our method can also be used for time-dependent SDEs. Here we go into this topic in more detail. In terms of implementation, one can consider a similar conditional generation model as in (7), with some modifications:

- The mapping  $f$  in (8) and the prior  $\gamma$  should depend on  $t$ .
- Equation (9) should be rewritten as (18), which implies that (10) becomes

$$p_\mu(Z_{t_2}|Z_{t_1}, t_1) = \frac{1}{\sqrt{2\pi(t_2 - t_1)}^d} \exp\left(-\frac{\|Z_{t_2} - Z_{t_1} - \mu(Z_{t_1}, t_1)(t_2 - t_1)\|^2}{2(t_2 - t_1)}\right).$$

- The encoder should also depend on time.

Besides implementation details, the results on identifiability also hold. Modifying Theorems 3 and 4 to accommodate time-dependent drift coefficients is not hard, you can see Theorem C.7 for an example on how Theorem 3 is also valid for time-dependent SDEs. Regarding Theorem 2 the crucial part is extending [12, Proposition 1]. Followingly, we present a version of [12, Proposition 1] that is valid also for time-dependent SDEs, followed by its proof.

**Theorem C.5** (Multivariate Lamperti transform). *Suppose that  $\{Y_t\}_{t \in \mathbb{T}} \in \mathbb{R}^d$  is a solution to the SDE:*

$$dY_t = \mu(Y_t, t) dt + \sigma(Y_t, t) dW_t, \quad (\text{C.1})$$

where  $\mu : \mathbb{R}^d \times \mathbb{T} \rightarrow \mathbb{R}^d$  and  $\sigma : \mathbb{R}^d \times \mathbb{T} \rightarrow \mathbb{R}^{d \times d}$ . Moreover, suppose the following conditions are satisfied:

(i)  $\mu$  and  $\sigma$  are globally Lipschitz, that is, (4) holds, and  $\sigma(y, t)$  is symmetric positive definite for all  $y \in \mathbb{R}^d, t \in \mathbb{T}$ .

(ii)  $\sigma$  is differentiable everywhere and for all  $y \in \mathbb{R}^d, t \in \mathbb{T}$  and  $j, k \in \{1, \dots, d\}$

$$\frac{\partial \sigma(y, t)}{\partial y_k} \sigma(y, t)^{-1} e_j = \frac{\partial \sigma(y, t)}{\partial y_j} \sigma(y, t)^{-1} e_k, \quad (\text{C.2})$$

where  $e_j$  is the  $j$ -th canonical basis vector of  $\mathbb{R}^d$ .

Then there exists a function  $g : \mathbb{R}^d \times \mathbb{T} \rightarrow \mathbb{R}^d$  and  $\tilde{\mu} : \mathbb{R}^d \times \mathbb{T} \rightarrow \mathbb{R}^d$  such that  $Y_t = g(Z_t, t)$  and  $\{Z_t\}_{t \in \mathbb{T}}$  is a solution to the SDE:

$$dZ_t = \tilde{\mu}(Z_t, t) dt + dW_t, \quad (\text{C.3})$$

*Proof.* We prove the lemma by constructing the functions  $g$  and  $\tilde{\mu}$  such that the SDE that governs  $Y_t = g(Z_t, t)$  is given by (C.1). By Ito's lemma [11], we have

$$dY_t = \left( \frac{\partial g}{\partial t}(Z_t, t) + \frac{\partial g}{\partial y}(Z_t, t) \tilde{\mu}(Z_t, t) + \frac{1}{2} \Delta g(Z_t, t) \right) dt + \frac{\partial g}{\partial y}(Z_t, t) dW_t, \quad (\text{C.4})$$

where  $\frac{\partial g}{\partial y}(z, t)$  is the Jacobian of  $g$ , only in terms of  $y$ , and  $\Delta g$  is the Laplacian, defined by

$$(\Delta g(z, t))_i = \sum_{k=1}^d \frac{\partial^2 g(z, t)_i}{\partial y_k^2}.$$

We now choose  $h$  and  $g$  as in Lemma C.6, noting that  $h$  is the inverse of  $g$ , therefore  $Z_t = h(Y_t, t)$  and

$$\begin{aligned} \frac{\partial g}{\partial y}(Z_t, t) &= \frac{\partial g}{\partial y}(h(Y_t, t), t), \\ &= \sigma(Y_t, t). \end{aligned}$$

We just obtained that the diffusion terms in (C.1) and (C.4) are equal, and the drift terms coincide if we define

$$\tilde{\mu}(z, t) := \frac{\partial g}{\partial y}(z, t)^{-1} \left( \mu(g(z, t), t) - \frac{\partial g}{\partial t}(z, t) - \frac{1}{2} \Delta g(z, t) \right).$$

□

**Lemma C.6.** *Suppose  $\sigma$  follows conditions (i) and (ii) in Theorem 2 and define*

$$h(y, t) := \int_0^1 \sigma(\tau y, t)^{-1} y \, d\tau. \quad (\text{C.5})$$

Then the following conditions hold:

(i)

$$\frac{\partial h}{\partial y}(y, t) = \sigma(y, t)^{-1}. \quad (\text{C.6})$$

(ii) *There exists a function  $g : \mathbb{R}^d \times \mathbb{T} \rightarrow \mathbb{R}^d$  such that for all  $z \in \mathbb{R}^d, t \in \mathbb{T}$ ,  $g(z, t) = y$  whenever  $h(y, t) = z$ .*

(iii)  *$g$  is differentiable everywhere and*

$$\frac{\partial g}{\partial y}(h(y, t), t) = \sigma(y, t).$$

*Proof.* First, (C.2) implies that for all  $j, k$

$$\begin{aligned} \frac{\partial}{\partial y_k} (\sigma(y, t)^{-1}) e_j &= -\sigma(y, t)^{-1} \frac{\partial \sigma(y, t)}{\partial y_k} \sigma(y, t)^{-1} e_j \\ &= -\sigma(y, t)^{-1} \frac{\partial \sigma(y, t)}{\partial y_j} \sigma(y, t)^{-1} e_k, \\ &= \frac{\partial}{\partial y_j} (\sigma(y, t)^{-1}) e_k, \end{aligned}$$

and (i) follows from [19, Theorem 11.49]. We now prove that  $h(\cdot, t)$  is an one-to-one function, thus proving its inverse  $g(\cdot, t)$  exists and is well-defined.

We start by showing that for all  $t$  the set  $\mathcal{H}_M := \{y : \|h(y, t)\| \leq M\}$  is compact. Since  $h$  is continuous,  $\mathcal{H}_M$  is a closed set, thus it remains to prove it is bounded. Condition (i) in Theorem 2 implies not only that  $\sigma(y, t)$  is positive definite but also that its norm is bounded by  $\|y\|$ .

$$\|\sigma(y, t)\| \leq \|\sigma(y, t) - \sigma(0, t)\| + \|\sigma(0, t)\|, \quad (\text{C.7})$$

$$\leq D\|y\| + \|\sigma(0, t)\|, \quad (\text{C.8})$$

$$\leq \tilde{D}(1 + \|y\|), \quad (\text{C.9})$$

where  $\tilde{D} = \max\{D, \max_{t \in \mathbb{T}} \|\sigma(0, t)\|\}$ . This implies the eigenvalues of  $\sigma(y, t)$  are upper-bounded by  $(1 + \|y\|)\tilde{D}$ , and since  $\sigma(y, t)$  is a PSD matrix, the eigenvalues of its inverse are lower bounded by  $1/((1 + \|y\|)\tilde{D})$ , thus

$$w^T \sigma(y, t)^{-1} w \geq \frac{\|w\|^2}{(1 + \|y\|)\tilde{D}} \quad \text{for all } y, w \in \mathbb{R}^d. \quad (\text{C.10})$$

Applying this and the Cauchy-Schwarz inequality,

$$\begin{aligned}
\|y\| \|h(y, t)\| &\geq y^T h(y, t) \\
&= \int_0^1 y^T \sigma(\tau y, t)^{-1} y \, d\tau, \\
&\geq \int_0^1 \frac{\|y\|^2}{(1 + \tau\|y\|)\tilde{D}} \, d\tau, \\
&= \frac{\|y\|}{\tilde{D}} \log(1 + \|y\|).
\end{aligned}$$

Therefore, if  $M \geq \|h(y, t)\|$ , then  $M \geq \frac{1}{\tilde{D}} \log(1 + \|y\|)$ , thus

$$\|y\| \leq \exp(M\tilde{D}) - 1,$$

which proves  $\mathcal{H}_M$  is bounded. We now prove  $h$  is surjective. Let  $z \in \mathbb{R}^d$  and

$$y_* = \operatorname{argmin}_{y \in \mathcal{H}_{1+2\|z\|}} \|h(y, t) - z\|^2. \quad (\text{C.11})$$

Since  $\mathcal{H}_{1+2\|z\|}$  is compact, the minimum is achieved by a point in  $\mathcal{H}_{1+2\|z\|}$ , and this point is not in the boundary. Since by definition  $h(0, t) = 0$ , we have  $0 \in \mathcal{H}_{1+2\|z\|}$  and for any element  $w \in \partial\mathcal{H}_{1+2\|z\|}$

$$\begin{aligned}
\|h(w, t) - z\| &\geq \|h(w, t)\| - \|z\|, \\
&= 2\|z\| + 1 - \|z\|, \\
&> \|z\| = \|h(0, t) - z\|,
\end{aligned}$$

thus  $w$  does not achieve the minimum. Since the minimum is achieved by an interior point of  $\mathcal{H}_{1+2\|z\|}$  and  $h$  is differentiable,  $y_*$  is a critical point of (C.11). We then have

$$\begin{aligned}
0 &= \nabla \|h(y_*, t) - z\|^2, \\
&= 2 \frac{\partial h}{\partial y}(y_*, t)(h(y_*, t) - z), \\
&= 2\sigma(y_*, t)^{-1}(h(y_*, t) - z).
\end{aligned}$$

Since  $\sigma(y_*, t)^{-1}$  is non-singular, we must have  $h(y_*, t) = z$ , thus  $h$  is surjective. We now prove that  $h(y, t) \neq h(w, t)$  for all  $y, w \in \mathbb{R}^d$ . By the Fundamental Theorem of Calculus

$$\begin{aligned}
(w - y)^T (h(w, t) - h(y, t)) &= \int_0^1 (w - y)^T \frac{\partial h}{\partial y}(y + \tau(w - y), t)(w - y) \, d\tau, \\
&= \int_0^1 (w - y)^T \sigma(y + \tau(w - y), t)^{-1}(w - y) \, d\tau > 0,
\end{aligned}$$

where the last line follows from (C.10), thus  $h(y, t) \neq h(w, t)$ ,  $h$  is bijective, and  $g$  in (ii) is well defined. Finally, (iii) follows from the Inverse Function Theorem

$$\begin{aligned}
\frac{\partial g}{\partial y}(h(y, t), t) &= \frac{\partial h}{\partial y}(y, t)^{-1}, \\
&= \sigma(y, t).
\end{aligned}$$

□

## C.2 Interpretability for learnable diffusion coefficients

Here we present a result similar to Theorem 3, but considering a learnable diffusion coefficient. That is, we rewrite (10),

$$p_{\mu, \sigma}(Z_{t+\Delta t} | Z_t, t) = \frac{1}{(2\pi\Delta t)^{\frac{d}{2}} \det \sigma(Z_t, t)^{\frac{1}{2}}} \exp\left(-\frac{1}{2\Delta t} (Z_{t+\Delta t} - \lambda(Z_t))^T \sigma(Z_t, t)^{-1} (Z_{t+\Delta t} - \lambda(Z_t))\right). \quad (\text{C.12})$$

where  $\sigma(Z_t, t)$  is the diffusion coefficient and  $\lambda(Z_t) = Z_t + \Delta t \mu(Z_t, t)$ . We first state the result, then explain some of our reservations against it, and finally present its proof.

A brief note on notation: for a symmetric  $n \times n$  matrix  $M$ , we denote by  $\text{vecsym } M$ , a vector of dimension  $\binom{n+1}{2}$ , which consists of  $M$  flattened to a vector, such that the entries off-diagonal only appear once, and are multiplied by  $\sqrt{2}$ . This definition implies that, for 2 symmetric matrices  $A$  and  $B$ , we have  $\text{tr}(AB) = (\text{vecsym } A)^T \text{vecsym } B$ . Moreover, we denote by  $u \oplus v$  the concatenation of vectors  $u$  and  $v$ .

**Theorem C.7.** *Suppose that the true generative model with arbitrary diffusion coefficients has parameters  $\theta^* = (f^*, \mu^*, \sigma^*, \gamma^*)$ , and that the following conditions hold:*

1. *The set  $\{x \in \mathcal{X} | \psi_\epsilon(x) = 0\}$  has measure zero, where  $\psi_\epsilon$  is the characteristic function of the density  $p_\epsilon$  defined in (8).*
2.  *$f^*$  is injective and differentiable.*
3. *Letting  $N = \binom{n+1}{2} + n$ , there exist  $N + 1$  vectors  $z_0, \dots, z_N$  and scalars  $t_0, \dots, t_N$  such that the vectors  $\mathbf{\Lambda}_1 - \mathbf{\Lambda}_0, \dots, \mathbf{\Lambda}_N - \mathbf{\Lambda}_0$ , with*

$$\mathbf{\Lambda}_i := \text{vecsym}(\sigma(z_i, t_i)^{-1}) \oplus (-2\sigma(z_i, t_i)^{-1}(z_i - \mu(z_i, t_i))), \quad (\text{C.13})$$

*are linearly independent.*

*Then if  $\theta = (f, \mu, \sigma, \gamma)$  are other parameters that yield the same generative distribution, that is*

$$p_\theta(x_{t+\Delta t}, x_t) = p_{\theta^*}(x_{t+\Delta t}, x_t) \quad \forall x_{t+\Delta t}, x_t \in \mathbb{R}^n, \quad (\text{C.14})$$

*then  $\theta$  and  $\theta^*$  are equal up to an affine transformation. That is, there exists an invertible matrix  $A$  and a vector  $b$ , such that for all  $z \in \mathbb{R}^d$ :*

$$f(z) = f^*(Az + b), \quad (\text{C.15})$$

$$\mu(z, t) = A^{-1} \mu^*(Az + b, t) \quad \forall t \in \mathbb{T}, \quad (\text{C.16})$$

$$\sigma(z, t) = A^{-1} \sigma^*(Az + b, t) A^{-T} \quad \forall t \in \mathbb{T}, \quad (\text{C.17})$$

*and*

$$p_\gamma(z) = |\det A|^{-1} p_{\gamma^*}(Az + b). \quad (\text{C.18})$$

Before we show the details of the proof, we explain why we have chosen not to include this result in the main submission. The main reason is that condition 3, in theorem statement, is not satisfied for simpler diffusion coefficients, such as a constant diffusion coefficient. We felt our theory was not satisfactory if it did not apply for a simple Brownian motion, which is one of the most simple SDEs that exist.

Other issue is related to identifiability: first we lose uniqueness up to an isometry, getting an affine transformation, and then we lose the connection between SDEs arising from the Itô's lemma. Itô's lemma implies that employing a change of variable effectively leads to another SDE, and therefore we can never estimate the true latent variable up to this change of variables. However Theorem C.7 fails to capture this.

Nevertheless, as stated in Section 7, we intend in future work to study how to these issues can be fixed. We finally present the proof of this Theorem.

*Proof of Theorem C.7.* The proof is again very similar to the proof of Theorem 3. The 3 steps are the same as in the previous proof, and step (I) follows exactly in the same way, so we start on step (II).

## Step (II)

From Step (I), we have that for all  $x_t, x_{t+\Delta t}$  in  $\mathcal{X}$ ,

$$\begin{aligned} & \log \text{vol } J_{f_*^{-1}}(x_{t+\Delta t}) + \log \text{vol } J_{f_*^{-1}}(x_t) + \log p_{\mu_*, \sigma_*}(f_*^{-1}(x_{t+\Delta t}) | f_*^{-1}(x_t), t) + \log p_{\gamma_*}(f_*^{-1}(x_t)) \\ &= \log \text{vol } J_{f^{-1}}(x_{t+\Delta t}) + \log \text{vol } J_{f^{-1}}(x_t) + \log p_{\mu, \sigma}(f^{-1}(x_{t+\Delta t}) | f^{-1}(x_t), t) + \log p_{\gamma}(f^{-1}(x_t)). \end{aligned} \quad (\text{C.19})$$

Let

$$\lambda(x_t) = f^{-1}(x_t) - \mu(f^{-1}(x_t), t)\Delta t, \quad (\text{C.20})$$

$$\eta(x_t) = \sigma(f^{-1}(x_t), t)^{-1}\lambda(x_t), \quad (\text{C.21})$$

and define analogously  $\lambda_*(x_t), \eta_*(x_t)$ . Let  $z_t = f^{-1}(x_t)$ , and similarly for  $z_{t+\Delta t}$ . We then have

$$\begin{aligned} & \log p_{\mu, \sigma}(z_{t+\Delta t} | z_t, t) \\ &= -\frac{1}{2} \log \det \sigma(z_t, t) - \frac{1}{2\Delta t} (z_{t+\Delta t} - \lambda(x_t))^T \sigma(z_t, t)^{-1} (z_{t+\Delta t} - \lambda(x_t)), \\ &= -\frac{1}{2} \log \det \sigma(z_t, t) - \frac{1}{2\Delta t} (z_{t+\Delta t}^T \sigma(z_t, t)^{-1} z_{t+\Delta t} - 2z_{t+\Delta t}^T \eta(x_t) + \lambda(x_t)^T \eta(x_t)). \end{aligned}$$

We now write this as an augmented linear system. Let  $\mathcal{A}(z) = \text{vecsymb}(zz^T) \oplus z$ ,

$$\xi(x_t) = \text{vecsymb}(\sigma(f^{-1}(x_t), t)^{-1}) \oplus (-2\eta(x_t)), \quad (\text{C.22})$$

and define  $\xi_*(x_t)$  analogously. We have

$$z_{t+\Delta t}^T \sigma(z_t, t)^{-1} z_{t+\Delta t} = \langle \text{vecsymb}(z_{t+\Delta t} z_{t+\Delta t}^T), \text{vecsymb}(\sigma(z_t, t)^{-1}) \rangle,$$

thus

$$\begin{aligned} & \log p_{\mu, \sigma}(z_{t+\Delta t} | z_t, t) \\ &= -\frac{1}{2} \log \det \sigma(z_t, t) - \frac{1}{2\Delta t} (\langle \mathcal{A}(z_{t+\Delta t}), \xi(x_t) \rangle + \lambda(x_t)^T \eta(x_t)), \\ &= -\frac{1}{2} \log \det \sigma(f^{-1}(x_t), t) - \frac{1}{2\Delta t} (\langle \mathcal{A}(f^{-1}(x_{t+\Delta t})), \xi(x_t) \rangle + \lambda(x_t)^T \eta(x_t)). \end{aligned}$$

Finally define

$$\psi(x_t) = \text{vol } J_{f^{-1}}(x_t) + \log p_{\gamma}(f^{-1}(x_t)) - \frac{1}{2} \log \det \sigma(f^{-1}(x_t), t) - \frac{\langle \lambda(x_t), \eta(x_t) \rangle}{2\Delta t}, \quad (\text{C.23})$$

$$\varphi(x_{t+\Delta t}) = \text{vol } J_{f^{-1}}(x_{t+\Delta t}), \quad (\text{C.24})$$

and  $\psi_*$  and  $\varphi_*$  analogously. We finally have for all  $x_t, x_{t+\Delta t}$  in  $\mathcal{X}$ , an equation similar to (B.5).

$$\psi(x_t) - \frac{1}{2\Delta t} \langle \mathcal{A}(f^{-1}(x_{t+\Delta t})), \xi(x_t) \rangle + \varphi(x_{t+\Delta t}) = \psi_*(x_t) - \frac{1}{2\Delta t} \langle \mathcal{A}(f_*^{-1}(x_{t+\Delta t})), \xi_*(x_t) \rangle + \varphi_*(x_{t+\Delta t}). \quad (\text{C.25})$$

We now proceed in the same way as before to obtain a similar equality for all  $x_{t+\Delta t} \in \mathcal{X}$ .

$$\mathcal{A}(f_*^{-1}(x_{t+\Delta t})) = \Xi_*^{-T} \Xi^T \mathcal{A}(f^{-1}(x_{t+\Delta t})) + \Xi_*^{-T} \psi, \quad (\text{C.26})$$

with the exception that the invertibility of  $\Xi_*^T$  is now a consequence of condition 3 in the theorem statement. To prove  $\Xi_*^{-T} \Xi$  is invertible, let  $z_0, z_1, \dots, z_N \in \mathbb{R}^d$ , with  $N$  defined as in the theorem statement, such that the vectors  $\mathcal{A}(z_i) - \mathcal{A}(z_0)$ ,  $i = 1, \dots, N$  are linearly independent. We note that the entries of  $\mathcal{A}(z)$  are linear independent polynomials so finding such vectors is always possible. Let  $x_i = f_*(z_i)$ ,  $i = 0, \dots, N$ , define  $\mathbf{A}_*$  as the  $N \times N$  matrix with columns  $\mathbf{A}_{*,i}$

$$\mathbf{A}_{*,i} = \mathcal{A}(f_*^{-1}(x_i)) - \mathcal{A}(f_*^{-1}(x_0)),$$

and define  $\mathbf{A}$  analogously. Equation (C.26) implies

$$\mathbf{A}_* = \Xi_*^{-T} \Xi^T \mathbf{A}. \quad (\text{C.27})$$

Since  $\mathbf{A}_*$  is invertible by construction, so is  $\Xi_*^{-T} \Xi^T$ . From (C.26), we can now get a linear dependence between  $f_*^{-1}$  and  $f^{-1}$ . Let  $\nu(z) = f_*^{-1}(f(z))$ , then (C.26) implies that there are symmetric matrices  $M_i$ , vectors  $v_i$  and scalars  $c_i$  such that

$$\nu(z)_i = z^T M_i z + v_i^T z + c_i, \quad (\text{C.28})$$

and that there are symmetric matrices  $\tilde{M}_i$ , vectors  $\tilde{v}_i$  and scalars  $\tilde{c}_i$  such that

$$\nu(z)_i^2 = z^T \tilde{M}_i z + \tilde{v}_i^T z + \tilde{c}_i. \quad (\text{C.29})$$

Subtracting the square of (C.28) with the (C.29) for all  $z$  implies that  $M_i = 0$ ,  $\tilde{M}_i = v_i v_i^T$ ,  $\tilde{v}_i = 2c_i v_i$  and  $\tilde{c}_i = c_i^2$ . This and the invertibility of  $\Xi_*^{-T} \Xi^T$  finally imply that there is an invertible matrix  $A$  and a vector  $b$  such that for all  $x_{t+\Delta t}$

$$f_*^{-1}(x_{t+\Delta t}) = A f^{-1}(x_{t+\Delta t}) + b. \quad (\text{C.30})$$

### Step (III)

Equation (C.30) implies that for all  $z \in \mathcal{Z}$

$$\begin{aligned} f(z) &= f_*(f_*^{-1}(f(z))), \\ &= f_*(A f^{-1}(f(z)) + b), \\ &= f_*(Az + b). \end{aligned}$$

Moreover  $J_f = J_{f_*} A$ , and  $\log \text{vol } J_{f^{-1}} = \log \text{vol } J_{f_*^{-1}} + \log |\det A|$ . Now replacing  $x_{t+\Delta t}$  by  $f(z)$  on (C.25) and using (C.30) and (C.23), we get for all  $z \in \mathcal{Z}$  and  $x_t \in \mathcal{X}$

$$\begin{aligned} \psi(x_t) - \frac{1}{\Delta t} \langle z, \eta(x_t) \rangle + \frac{z^T \sigma(f^{-1}(x_t), t)^{-1} z}{2\Delta t} + \log |\det A| \\ = \psi_*(x_t) - \frac{1}{\Delta t} \langle Az + b, \eta_*(x_t) \rangle + \frac{(Az + b)^T \sigma_*(f_*^{-1}(x_t), t)^{-1} (Az + b)}{2\Delta t} \end{aligned} \quad (\text{C.31})$$

Taking derivatives with respect to  $z$ , we get

$$-\eta(x_t) + \sigma(f^{-1}(x_t), t)^{-1} z = -A^T \eta_*(x_t) + A^T \sigma_*(f_*^{-1}(x_t), t)^{-1} (Az + b) \quad (\text{C.32})$$

Taking derivatives again we get

$$\sigma(f^{-1}(x_t), t)^{-1} = A^T \sigma_*(f_*^{-1}(x_t), t)^{-1} A \quad (\text{C.33})$$

Letting  $f(z) = x_t$  and using (C.30), we get for all  $z \in \mathcal{Z}$ ,

$$\sigma(z, t) = A^{-1} \sigma_*(Az + b, t) A^{-T} \quad (\text{C.34})$$

Replacing this back in (C.32), using (C.21) and multiplying by the inverse of (C.33), we get

$$\lambda(x_t) = A^{-1} \lambda_*(x_t) - A^{-1} b, \quad (\text{C.35})$$

or  $\lambda_*(x_t) = A \lambda(x_t) + b$ . Using (C.33), (C.20), letting  $f(z) = x_t$  and using (B.13), we get for all  $z \in \mathcal{Z}$ ,

$$Az + b - \mu_*(Az + b, t) \Delta t = Az - A \mu(z, t) \Delta t + b \quad (\text{C.36})$$

which implies  $\mu(z, t) = A^{-1} \mu_*(Az + b, t)$  for all  $z \in \mathcal{Z}$ . Finally, replacing all equations obtained in (C.31), and using (C.23), we get

$$\log p_\gamma(f^{-1}(x_t)) = \log p_{\gamma_*}(f_*^{-1}(x_t)) - \log |\det A|, \quad (\text{C.37})$$

and (C.18) follows from taking  $x_t = f(z)$  and using (C.30).  $\square$

## D. Calculating optimal orthogonal and affine transformations

Here we describe the minimizers of (19). Let  $A$  be a  $d \times N$  matrix with columns given by  $A_t = \tilde{f}^{-1}(X_t)$ , and let  $B$  a  $d \times N$  matrix with columns given by  $B_t = Z_t$ . Then we have (19) is equivalent to:

$$\mathcal{L}_{\text{latent}} = \frac{1}{N} \min_{Q,b} \|QA + b\mathbf{1}^T - B\|_F^2, \quad (\text{D.1})$$

where  $\mathbf{1}$  is the all-ones vector and  $\|\cdot\|_F$  denotes Frobenious norm, defined by  $\|M\|_F = \sqrt{\text{tr}(M^T M)}$ . Followingly, we use the Frobenious dot-product of matrices, defined as  $\langle M, O \rangle = \text{tr}(M^T O)$ . We present closed form solutions of

$$\begin{aligned} \min \|QA + b\mathbf{1}^T - B\|_F^2 \\ \text{s.t. } Q \in \mathbb{R}^{d \times d}, b \in \mathbb{R}^d \end{aligned} \quad (\text{D.2})$$

for both the cases where the optimization is over square matrices and over orthogonal matrices. We first calculate  $b$  (in terms of  $Q$ ).

$$\begin{aligned} \|QA + b\mathbf{1}^T - B\|_F^2 &= \|QA - B\|_F^2 + \langle b\mathbf{1}^T, b\mathbf{1}^T - 2(QA - B) \rangle \\ &= \|QA - B\|_F^2 + \text{tr}(\mathbf{1}b^T(b\mathbf{1}^T - 2(QA - B))) \\ &= \|QA - B\|_F^2 + \text{tr}(Nb^Tb - 2b^T(QA - B)\mathbf{1}) \end{aligned}$$

We see this is a convex function over  $b$ , so we get the minimum by finding the critical points. Equating the gradient of  $b$  to zero, we get

$$\begin{aligned} 2Nb - 2(QA - B)\mathbf{1} &= \mathbf{0} \\ \Rightarrow b &= \frac{1}{N}(QA - B)\mathbf{1} \end{aligned} \quad (\text{D.3})$$

Replacing  $b$  in (D.2), we get

$$\min_Q \|Q\tilde{A} - \tilde{B}\|_F^2, \quad (\text{D.4})$$

where  $\tilde{A} = A - \frac{1}{N}A\mathbf{1}\mathbf{1}^T$  and  $\tilde{B} = B - \frac{1}{N}B\mathbf{1}\mathbf{1}^T$ . We note that  $\frac{1}{N}A\mathbf{1}$  and  $\frac{1}{N}B\mathbf{1}$  are the average of the columns of  $A$  and  $B$ , respectively, thus  $\tilde{A}$  and  $\tilde{B}$  are centered versions of  $A$  and  $B$ .

We first find the minimum of (D.4) for general square matrices. In this case the objective is again a convex function of the entries of  $Q$ , so we can find the minimizer by equating the gradient of  $Q$ .

$$\begin{aligned} 2Q\tilde{A}\tilde{A}^T - 2\tilde{B}\tilde{A}^T &= \mathbf{0} \\ \Rightarrow Q &= \tilde{B}\tilde{A}^T(\tilde{A}\tilde{A}^T)^{-1} \end{aligned}$$

On the other hand, if  $Q$  is orthogonal, then (D.4) is an instance of the orthogonal Procrustes problem [20], and letting  $USV^T = \tilde{B}\tilde{A}^T$  be the singular value decomposition of  $\tilde{B}\tilde{A}^T$ , the minimizer is  $Q = UV^T$ .

Finally, with  $Q$  calculated, we replace it in (D.3) to finally calculate  $b$ .

## E. Cramer-Rao bounds for estimating the drift coefficient

Here we derive the Cramér-Rao lower bound (CRLB) we use for estimating SDEs. The CRLB gives an information theoretically lower bound on the MSE of any estimator, and in particular it is also a lower bound for estimating  $\mu$  using the proposed VAE. However, it is hard to calculate the CRLB for some of the SDEs considered, thus we focus on the simplified problem: determining  $\mu$  up to a global shift. That is,

$$\mu(z) = \mu^*(z) + \eta, \quad \forall z \in \mathcal{Z},$$

where the function  $\mu^*(z)$  is known but  $\eta \in \mathbb{R}^d$  is unknown. We note that this is the exact CRLB for the constant drift SDE, and is still a lower bound on the estimation error for the OU process.

Using the Euler-Maruyama approximation, the increments of the SDE are distributed as  $\mathcal{N}((\mu^*(z) + \eta)\Delta t, \sigma\Delta t)$ . The CRLB for an estimator of the mean  $\hat{\mu}$  of the Gaussian distribution  $\mathcal{N}(\mu, \sigma)$  is

$$\text{Cov}(\hat{\mu}) \succeq \frac{1}{N}\sigma,$$

which implies that  $\mathbb{E}[\|\hat{\mu} - \mu\|^2] \geq \frac{1}{N} \text{tr} \sigma$ . Substituting the values from our increment distribution, and taking into account that  $\sigma = I$ , we get

$$\begin{aligned} \mathbb{E}[\|(\hat{\eta} - \eta)\Delta t\|^2] &\geq \frac{\text{tr}(I)\Delta t}{N} \\ \mathbb{E}[\|\hat{\mu}(z) - \mu(z)\|^2] &\geq \frac{d}{\Delta t N} \end{aligned}$$

Replacing the values of  $d$ ,  $\Delta t$  and  $N$  we get the CRLB values on the last column of Table 1.

## F. Experiment Details

### F.1 Architecture

The architecture used for all experiments with the proposed method is delineated in Table F.3. It is based on the architecture described in the Supplemental Material of [21]. In the balls experiments  $d = 2$ , in the digits is  $d = 4$ , and Wasserstein is  $d = 1$ . We define these operations for the architecture:

- $\text{FC}(n_{in}, n_{out})$ : Fully connected layer with input/output dimensions given by  $n_{in}$  and  $n_{out}$ .
- $\text{Conv}(n_{in}, n_{out}, k, s, p)$ : Convolutional layer with input channels  $n_{in}$ , output channels  $n_{out}$ , kernel size  $k$ , stride  $s$  and padding  $p$ .
- $\text{MaxPool}(k, s, p)$ : Maximum Pooling with kernel size, stride and padding respectively given by  $k$ ,  $s$  and  $p$ .
- $\text{BN}$  : Batch-normalization.
- $\text{U}$  : 2D upsampling bilinear interpolation layer.

Encoder	Decoder
Input size: (3, 64, 64)	Input size: ( $d$ , )
Conv(3, 8, 5, 1, 2), LeakyReLU, MaxPool(2, 2, 0)	FC( $d$ , 4096)
Conv(8, 16, 5, 1, 2), BN, LeakyReLU, MaxPool(2, 2, 0)	Unflatten
Conv(16, 32, 5, 1, 2), BN, LeakyReLU, MaxPool(2, 2, 0)	U, Conv(64, 64, 5, 1, 2), BN, LeakyReLU
Conv(32, 64, 5, 1, 2), BN, LeakyReLU	U, Conv(64, 32, 5, 1, 2), BN, LeakyReLU
Flatten	U, Conv(32, 16, 5, 1, 2), BN, LeakyReLU
FC $_{\mu}$ (4096, $d$ ), FC $_{\sigma}$ (4096, $d$ )	U, Conv(16, 8, 5, 1, 2), BN, LeakyReLU
Output size : ( $d$ , )	U, Conv(8, 3, 5, 1, 2), Sigmoid
	Output size : (3, 64, 64)

Table F.3: Encoder/Decoder architectures for experiments

Finally, the drift coefficient  $\mu$  is parameterized by a multi-layer perceptron with depth 4, width 16 and softplus activation function.

### F.2 Hyperparameters

The list of hyperparameters used for the MLP and parametric experiments are available in Table F.4 and Table F.5 respectively.

Dataset	Balls		Digits		Wasserstein
Experiment	Walk	OU	Walk	OU	OU
Batch Size	200		100		200
AE LR	0.0001	0.001	0.0002		0.0001
$\mu$ LR	0.0001	0.001	0.0002		0.0001
Optimizer	Adam				
Epochs	4000		2500		10000

Table F.4: Hyperparameters for MLP experiments.

Dataset	Balls		Digits		Wasserstein
Experiment	Walk	OU	Walk	OU	OU
Batch Size	800	200	100		200
AE LR	0.0004		0.0004		0.0001
$\mu$ LR	0.002		0.0004		0.0001
Optimizer	Adam				
Epochs	2000	4000	2500		10000

Table F.5: Hyperparameters for parametric experiments.

## F.2 Parameterization

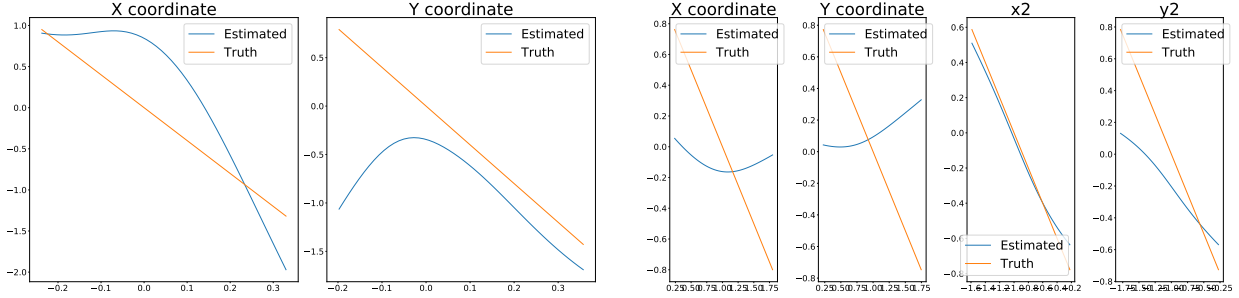
For the random walk, there was one parameter for each of the variables in the latent space,  $\mu_i = a_i$ . For the OU, we parameterized  $\mu_i = a_i x_i$  where  $a_i$  is a scalar and  $x_i$  is the latent variable for dimension  $i$ .

## F.3 Training notes

The MLP was initialized with Xavier initialization with gain 0.5. The encoders and decoders were initialized using Kaiming initialization. All other parametric experiments were initialized using normally distributed random variables. In the MLP experiments, exponential learning rate decay was applied at a rate of 0.99999, no decay was applied in the parametric experiments. All experiments were validated using a 100 sample hold-out sequence subset of the data, and the best validation loss was chosen for the network parameters. A 100 sample test sequence was also held out for testing reconstruction capabilities. These were chosen to be the last 200 points in each run. In practice, reserving data for validation seemed to not be as important, since most times the network obtained in the last epoch was generally sufficient. The parameters were chosen manually by observing the validation loss. Differences in hyperparameters are due to the learning dynamics of the latent network versus the few parameters, and validation data was crucial to assess these learning dynamics. The final parameters were chosen as the best out of the total number of epochs where the product of the loss terms is minimized.

### F.3.1 Sensitivity to hyperparameters

When optimizing with the MLP as the approximation of  $\mu$ , the final output is sensitive to the weight initialization and other hyperparameters. This is expected since there is limited data and the MLP can easily overfit to a limited set of data. In this case, we choose not to regularize the MLP with additional weight penalties or Sobolov norms due to the estimator becoming biased and the CRLB not being valid. However, in practice adding such regularization would likely lead to better estimates of  $\mu$ . In general, if a parametric form can be assumed for the underlying SDE, this should be used since the estimates are best for that case. From our experiences, the best approach is to perform a grid search over a set of learning rates for the encoder and decoder and  $\mu$  and choose the best one based on a validation subset. Further analysis is needed to understand the training dynamics and impose a more rigorous training strategy. Finally, when considering a parametric case, finding the least squares solution after a number of warm-up iterations may provide good starting points for the SDE. All of these approaches can be explored in future work.



(a) Example of the Ball OU case where the MLP overfits to the observed data;

(b) Example of the MNIST OU case with the MLP for  $\mu$  where two components are recovered fairly well but the other two are not.

Figure F.4: Examples of overfitting.

## F.4 Failure Cases

Here we describe some of the failure modes that can be mitigated using differences in hyperparameters.

### F.4.1 Reconstruction Quality

For certain cases, particularly in MNIST, the quality of the image reconstructions are not very good. The parameter that enforces this quantity is the variance parameter for the decoder. We suggest tuning this parameter based on a validation set to find the optimal parameter.

### F.4.2 Nonparametric Fitting

In the cases described in the paper, we consider the MSE because of its relationship to the CRLB. However, the MSE does not accurately describe the topology of  $\mu$  or how it has overfit to the data. Adding additional regularizers to the function may prevent this which we leave this as a choice to the user. Some examples of failures are available in Figure F.4. While this does happen, the averages reported suggest the proposed method is fairly close to the lower bound in most cases.

## F.5 Comparison Notes

While we could not find any methods that directly support stochastic data in the manner that we are proposing, the methods we did consider were primarily developed for video prediction tasks. In the original experiments of the compared methods, the motion of the data was significantly smoother than the data used here and the quantity of data was much larger. These are the reasons we believe contribute to the lack of effectiveness of the compared methods. While training for both methods, we tried to modify the training procedure to account for the differences in the data. For the ODE<sup>2</sup>VAE, we trained on the full sequence as required through the latent adjoint method based on the PyTorch implementation provided at <https://github.com/cagatayildiz/ODE2VAE>. The encoder decoder architecture for ODE<sup>2</sup>VAE was the same as in Table F.3. We also tried a grid search over the learning rate to obtain better results, but we could not see a significant difference in the output over different learning rates. When training over the full sequence for DDPAE, we noticed samples were visually blurry, so we opted to only train on one frame and predict the next frame. For DDPAE, we modified the parameters from the implementation available in <https://github.com/jthsieh/DDPAE-video-prediction> to accommodate the smaller dataset. Initial experiments with default parameters proved to be difficult to train.

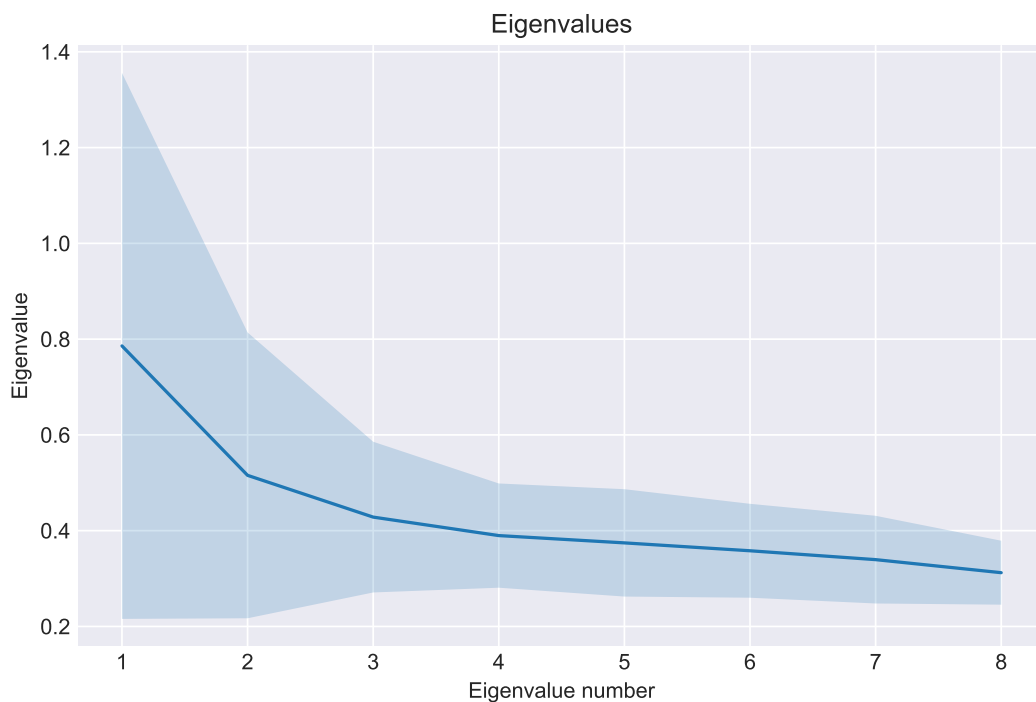


Figure F.5: Distribution of eigenvalues for random walk with latent dimension 8 and SDE dimension 2. Shaded region represents one standard deviation from the values of 5 runs.

## F.6 Unknown Latent Dimension

Here we provide a simulation of a ball moving according to an SDE only along one dimension while maintaining a higher dimensional latent space. The plot of the eigenvalues of the estimated  $\Sigma$  matrix suggests the model is learning the lower dimensional representation.

## F.7 Computational Resources

Models were trained on an NVIDIA GeForce RTX-2080 Ti and a NVIDIA GeForce Titan RTX graphics card. All code was implemented in PyTorch.